CIRP Annals - Manufacturing Technology 63 (2014) 727–749

Contents lists available at ScienceDirect

CIRP Annals - Manufacturing Technology

journal homepage: http://ees.elsevier.com/cirp/default.asp

Testing and modelling of material behaviour and formability in sheet metal forming

S. Bruschi (2)[a,*], T. Altan (1)[b], D. Banabic (2)[c], P.F. Bariani (1)[a], A. Brosius[d], J. Cao (2)[e], A. Ghiotti[a], M. Khraisheh (2)[f], M. Merklein (2)[g], A.E. Tekkaya (1)[h]

[a] DII, University of Padova, Via Venezia 1, 35131 Padova, Italy
[b] Ohio State University, Columbus, OH, USA
[c] Technical University of Cluj Napoca, Cluj Napoca, Romania
[d] Chair of Forming and Machining Processes, TU Dresden, Dresden, Germany
[e] Northwestern University, USA
[f] Qatar Environment and Energy Research Institute, Qatar Foundation, Qatar
[g] LFT, Friedrich-Alexander-Universität Erlangen-Nürnberg, Erlangen, Germany
[h] Technische Universität Dortmund, Dortmund, Germany

ARTICLE INFO

Keywords:
Sheet metal
Forming
Modelling

ABSTRACT

The paper deals with the testing and modelling of metals response when subjected to sheet forming operations. The focus is both on the modelling of hardening behaviour and yield criteria and on the description of the sheet metal formability limits. Within this scope, the paper provides a critical review of the models available today for predicting the material behaviour at both industrial and scientific level, and the tests needed to identify the models' material parameters. The most recent advances in the field are also presented and discussed with particular emphasis on the challenges the sheet metal forming community is now facing.

1. Background and introduction

1.1. Material response and related phenomena

In sheet metals, the response to plastic deformation manifests itself through different phenomena, such as hardening, anisotropy, failure and fracture. Most of these phenomena occur simultaneously with significant interactions and may deeply affect the behaviour of the sheet metal due to the significant changes they cause in its physical and mechanical features and properties, such as surface appearance and roughness, yield-point elongation, resistance to plastic deformation, hardness and strength, residual stresses and geometric distortion, springback, and formability.

In the scientific and technical literature, testing and modelling of material behaviour in sheet metal forming are dealt with separately from bulk metalworking. Even if metal sheets are products of a bulk deformation, namely rolling, the deformation mostly occurs by tensile forces in the plane of the sheet rather than by compression and the mechanics of sheet forming basically consists of stretching and bending. Furthermore, material properties that are of primary importance to sheet-metal forming are somewhat different from those of bulk forming, since the appearance and surface integrity of the formed sheets, for example, pose a major concern.

1.2. Value of modelling

Virtual prototyping tools of processes and systems in the domain of sheet metal working is nowadays a real prospect for industrial users to provide accurate predictions of the part geometrical features and post-forming characteristics (e.g. residual stresses) and possible defects and failures on the basis of the chosen process parameters. Thanks to these predictions, critical decisions in process design are taken, strongly affecting the technical and economical success of the process, such as the selection of the proper process chain, the tool and equipment design, the process design with respect to the product service life characteristics. However, to make the numerical simulation tools reliable and versatile for efficiently and accurately predicting the events and phenomena that materials, processes and products are subjected to, useful and efficient models and tests able to evaluate the different aspects of the material response to deformation are among the most critical prerequisites.

The variety of material response models currently utilized differ from one another in the length scale of the phenomena they describe, origin and nature of their formulation and aspects of the material behaviour they focus on. Their predictive capability depends on the accuracy, consistency and transferability of their predictions as well as on the versatility of their structure. Many of the considerations reported in [35,74,107] on the categorization and capabilities of predictive models for the technological domain of bulk deformation and on the

* Corresponding author.

http://dx.doi.org/10.1016/j.cirp.2014.05.005
0007-8506/© 2014 CIRP.

prerequisites for their successful application may apply to the domain of sheet forming processes.

Each model has its precise requirements in terms of experimental data and testing needed to identify its parameters, generate its database and carry out its validation. The availability of reliable data and suitable equipment for testing are, together with the costs for experiments and computations for data generation, often decisive factors in whether or not a model is used and successfully applied.

Even though new models and tests continue to be proposed, most of the applications of both the existing and new ones remain, with very few exceptions, at the research level. The use of these models, in fact, requires significant scientific and specialized knowledge, and process designers in industry rarely, if ever, use them.

1.3. Paper scope and objective

This paper deals with the testing and modelling of the different phenomena that take part in the response of metals when they undergo plastic deformation in an industrial sheet forming operation. The tests and models considered in the paper are relevant to all the main aspects of the material behaviour, including failure and fracture phenomena.

Within this scope, the main aim of this paper is to present what models and tests are available today, together with their limitations, and to identify the most recent applications and developments to meet the special requirements of the sheet metal forming industry. The emphasis is on what is changing and still needs changing in order to provide process designers with more useful and efficient models that can meet the increasing demand for accurate process and product simulations. Therefore, the aim of the paper is to provide an exhaustive and systematic review of the plethora of models and relevant tests that are available today.

Taking this into account, the paper is organized into three main parts. In the first part (Section 2), models devoted to the representation of hardening behaviour, yield criteria and formability limits are reviewed, emphasizing the current trend from phenomenological to physical modelling. In the second part (Section 3), tests devoted to the identification of the material parameters of the models previously reported are described on the basis of their capabilities to reproduce the sheet metal forming operating conditions. Finally, in the third part (Section 4) there is a short outlook of what future developments may be expected, and some suggestions for further research are given.

2. Models of material behaviour and forming limits of sheet metals

The numerical simulation of a sheet forming process requires the implementation of two categories of models: (i) models that characterize the flow behaviour of the sheet metal, and (ii) models that predict the sheet metal forming limits under specific processing conditions. The first category comprises hardening models and yield criteria, as the description of the behaviour of a sheet metal in a multi-axial stress space needs an accurate representation of the following three elements: (i) a yield criterion, correlating the stress components when the yielding occurs; (ii) a flow rule, connecting the components of the strain-rate and stress; (iii) a hardening rule, describing the evolution of the initial yield locus. The second category includes phenomenological and physical models of the sheet metal forming limits, testifying an evolutionary trend from empirical curve fitting to theoretically-based models that describe the causes of the sheet metal failure. These two categories of models are reviewed in this section, with a brief analysis of the state of development, their distinct features of evolution, their value and limits of their application. The section includes also a chapter dedicated to the modelling of phase transformation and microstructural features evolution, particularly important for the accurate description of the response to deformation of the emerging classes of sheet metals during conventional and innovative forming processes.

2.1. Modelling of hardening

The first attempts to model the sheet metal hardening were based on scalar phenomenological models, involving the uniaxial loading of the metal sheet at room temperature under one loading path. However, the conditions experienced in real forming operations require an extension of this simple approach to describe the effects of cyclic loading and non-linear strain paths, making the hardening models evolve from the first scalar phenomenological approach to physical approaches, capable of fully describing the hardening through the modelling of the physical phenomena that characterize the metal sheet behaviour.

2.1.1. Phenomenological modelling of hardening

Four typologies of hardening may arise during sheet forming processes (Fig. 1): (i) isotropic hardening, which refers to the proportional expansion of the initial yield surface; (ii) kinematic hardening, if the deforming material shows a yield surface that does not change in form and size, but translates in the stress space; (iii) rotational hardening, which causes the yield locus to rotate; (iv) distortional hardening, which causes the yield locus to distort.

Isotropic hardening laws are suitable for describing the sheet metal behaviour under monotonous processes during which the load direction does not change. The description of the isotropic hardening indicating the proportional expansion of the sheet metal initial yield surface is fulfilled according to Eq. (1):

$$f = f_y(\boldsymbol{\sigma}) - \sigma_y(\varepsilon^p) \tag{1}$$

where f is the current yield surface, f_y is the expression for yielding proposed by the different yield criteria, and $\sigma_y(\varepsilon^p)$ is the flow stress as a function of the plastic strain. This last term is usually described through phenomenological models based on power laws, such as the ones from Hollomon [115], Swift [212] and Ludvik [163], or modifications of them that take into account a saturation term for the flow stress, such as the ones from Voce [234] and Hockett and Sherby [114]. The material parameters of the isotropic hardening models are identified on the basis of experimental data obtained from monotonic test methods, mainly uniaxial tensile tests.

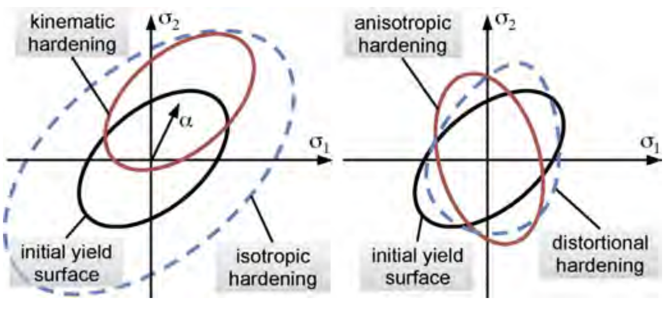

Fig. 1. Evolution of the yield locus according to hardening types.

Isotropic hardening models overestimate the hardening in reversal loading resulting in overestimation of the predicted springback and residual stresses. Reversal loading commonly occurs in sheet metal forming operations leading to different phenomena, namely the Bauschinger effect, smooth elasto-plastic transient behaviour, permanent softening and stagnation behaviour (the latter especially in case of mild steel sheets) (Fig. 2).

The Bauschinger effect, first detected in [40], indicates a reduced yield stress of the sheet metal upon load reversal (point c′ instead of c in Fig. 2). This effect can be described by kinematic hardening laws, which state that the initial yield surface translates in the stress space according to Eq. (2):

$$f = f_y(\boldsymbol{\sigma} - \boldsymbol{\alpha}) - k^2 \tag{2}$$

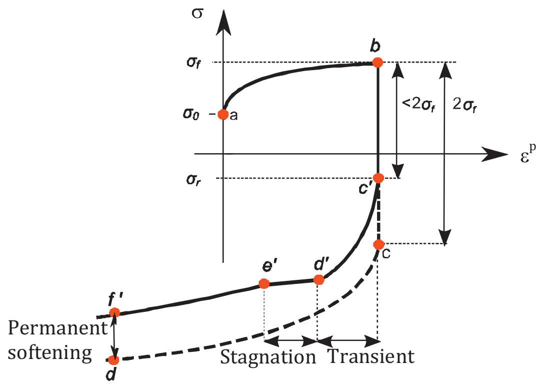

Fig. 2. Hardening curve in case of a reversed loading condition.

where α is the kinematic or back stress tensor, namely the representation of the yield locus translation in the stress space, and k is the initial yield stress. The first linear kinematic hardening models able to capture the Bauschinger effect were proposed by Prager [195] and Ziegler [251], the former assuming the yield surface translating in the same direction of the plastic strain, the latter radially from the centre.

However, the linear kinematic hardening laws result in yielding at very low stress during reverse loading, over-predict the softening behaviour, and cannot represent the hardening non-linearity. The transient behaviour, depicted as a rapid change in the strain hardening rate from the elastic to the plastic region (segment c′–d′ in Fig. 2), was first described by non-linear kinematic hardening laws, based on the formulation proposed by Armstrong and Frederick [9] according to Eq. (3):

$$\dot{\boldsymbol{\alpha}} = C_X\left(\frac{\alpha_{sat}}{\bar{\sigma}_0}(\boldsymbol{\sigma}' - \boldsymbol{\alpha}) - \boldsymbol{\alpha}\right)\dot{\bar{\varepsilon}} \tag{3}$$

where α is the kinematic or back stress tensor, σ' the deviator of the Cauchy stress tensor, and C_X and α_{sat} are material parameters that can be identified from cyclic tests [9].

A combination of the isotropic and kinematic hardening models, named mixed hardening, provides a yield surface expanding uniformly in shape and translating in the stress space, which is modelled according to Eq. (4):

$$f = f_y(\boldsymbol{\sigma} - \boldsymbol{\alpha}) - \sigma_y(\varepsilon^p) \tag{4}$$

where $\sigma_y(\varepsilon^p)$ is the stress–strain relation.

Currently, two classes of models are the most widely accepted in the sheet metal forming to describe the mixed hardening behaviour. The first class is based on the model proposed by Chaboche [58,59] as a modification of the Armstrong and Frederick's model, which was able to capture also the permanent softening behaviour (between f′ and d in Fig. 2). The Chaboche's approach was later on adopted and enhanced by other researchers [54,62,86,135].

The second class of models refers to the two-surface models proposed by Krieg [142], Dafalias and Popov [66], McDowell [172], and Lee [154], which define the continuous variation of hardening between two surfaces, the yield and the bounding ones, and can capture the transient and softening behaviours. The bounding surface F is represented by the Eq. (5):

$$F(\boldsymbol{\Sigma} - \mathbf{A}) - \bar{\Sigma}_{iso} = 0 \tag{5}$$

where Σ and $\mathbf{A}$ are the stress and back stress of the bounding surface, and $\bar{\Sigma}_{iso}$ is the size of the bounding surface.

Assuming that the bounding surface F and the yield surface f have the same shapes and surface normal directions, the two surfaces move relatively along the direction $\Sigma - \sigma$, the back stress of the bounding surface $\mathbf{A}$ becomes Eq. (6):

$$d\mathbf{A} = d\boldsymbol{\alpha} - d\mu(\boldsymbol{\Sigma} - \boldsymbol{\sigma}) = d\mathbf{A}_1 - d\mathbf{A}_2 \tag{6}$$

The two surfaces model proposed by Yoshida and Uemori [246] makes the yield surface translate within the bounding surface, while the bounding surface translates and expands uniformly in shape; this model can also describe the work hardening stagnation (segment d′–e′ in Fig. 2), and requires a relatively low number of material parameters to be identified.

Recently, an attempt to unify various modelling approaches was proposed in [240], where a thermodynamic approach is used, though its mathematical complexity may prevent the practical application.

2.1.2. Physical modelling of hardening

Nonetheless the capabilities of the Yoshida and Uemori's model to fully describe the hardening curve upon load reversal, it cannot describe the anisotropic and distortional hardening behaviour. The former is due to the change of the sheet metal plastic anisotropy at increasing level of deformation as a consequence of the texture evolution; in addition, in case of non-proportional loading with abrupt changes of the loading path (e.g. orthogonal strain paths), relevant in most multi-stage forming processes, the yield surface presents a region of high curvature roughly in the loading direction and a flattening region in the opposite direction, which provokes a distortional hardening that cannot be neglected. The simplest generalizations of the Chaboche's model to account for the distortional hardening are based on the use of second-rank back stress-like tensors, which allow the orientation of the yield surface following the loading path so that the change of the loading direction leads to a reorientation of the yield surface.

A more comprehensive description of such behaviour is given by the dislocation-based microstructural model proposed by Teodosiu and Hu [219], which were the first to propose a physically-based hardening model, which describes the sheet metal anisotropic hardening behaviour induced by microstructural evolution at large strain. This model describes the hardening by four internal state variables, namely R, P, X and S, which, in turn, describe respectively the material isotropic hardening induced by randomly accumulated dislocations, the polarity of planar dislocation structures, the rapid changes in stress under strain-path changes, and the directional strength of planar dislocation structures [103]. Thirteen material parameters need to be identified on the basis of the results from different tensile and shear tests with various strain path changes. A number of other models, based on that of Teodosiu and Hu, have been recently developed to account for the anisotropic hardening effects in non-proportional strain paths [44,160]. Alternatively, polycrystalline models can be effective in predicting the sheet metal behaviour under complex load paths: since the distortion of the yield surface is related to the activation and cross-hardening of different slip systems depending on the metal crystallographic orientations, the physical phenomenon can be adequately described by this class of models [204].

2.1.3. Modelling of hardening at elevated temperature and/or high strain rate

Varying strain rates and different temperature levels can have a discernable influence on the hardening behaviour. In the past, these effects were of minor interest in forming technology. However, more recently, with the introduction of new materials dedicated to sheet forming such as advanced high strength steels, magnesium and titanium alloys, as well as processes like hot stamping or electro-magnetic forming conducted at either elevated temperature or high strain rate, they have become much more relevant. In general, high strain rates lead to higher flow stresses, while high temperatures reduce the required stress level. However, the definition of 'high strain rate' and 'high temperature' depends on the process itself and related effects, and should be defined accordingly.

A review of the laws to describe the sheet metal behaviour at elevated temperature is given in [132]: the Johnson-Cook [127], Norton-Hoff, and Voce–Kocks are the ones most widely used, each of them providing the direct dependency of the flow stress on the strain, temperature, and strain rate. However, all these models assume the sheet metal isotropic behaviour. To account for the sheet metal anisotropic behaviour, a new approach was presented in [144], where a model taking into account the sheet anisotropic behaviour and hardening as a function of the temperature and strain rate was developed and implemented into a non-commercial code for the simulation of the forming of Al–Mg alloy sheets under warm conditions.

2.1.4. The value and limits to hardening models

The isotropic and kinematic hardening models still dominate the industrial practise, mainly due to their inherent simplicity, ease in calibration through uniaxial and proportional loading cyclic tests, and capacity to predict the sheet metal behaviour under monotonic and reversal loadings. However, the description of the sheet metal behaviour under complex strain paths, as in multi-step forming processes, leads to an increase in the level of complexity of the hardening models, from phenomenological to physical approaches, which, in turn, need to be calibrated on the basis of advanced testing techniques, comprising multi-axial tests. Additionally, those hardening models that are function of temperature and strain rate require a huge experimental effort to account for the effects of temperature and strain rate, even if uniaxial and monotonic loading testing conditions are applied.

2.2. Yield criteria

The yield criteria define the condition for the elastic behaviour limit under multi-axial states of stress, after which the material continues deforming plastically until failure, showing a hardening behaviour. Over the years, the modelling of the sheet metal yield criteria has evolved to describe more accurately the anisotropic behaviour, on the basis of the first yield criteria proposed for isotropic materials by Tresca [225], Huber [117] and Von Mises [184].

2.2.1. Anisotropic yield criteria

Hill proposed one of the first anisotropic yield criteria, the Hill48 quadratic criterion, which has the approximation of Eq. (7) for the plane stress case [111]:

$$\sigma_1^2 - \frac{2r_0}{1+r_0}\sigma_1\sigma_2 + \frac{r_0(1+r_{90})}{r_{90}(1+r_0)}\sigma_2^2 = \sigma_0^2 \tag{7}$$

where r_0 and r_{90} are the anisotropy coefficients at 0° and 90° with respect to the rolling direction, and σ_0 is the uniaxial yield stress in the rolling direction.

The Hill48 criterion cannot describe the behaviour of sheet metals with an r-value less than the unity and the yield stress σ_b under balanced biaxial tension significantly higher than the uniaxial yield stress σ_u in the plane of the sheet (or the reciprocal): this behaviour was observed in [238] for aluminium alloy sheets having an r-value between 0.5 and 0.6. To capture this "anomalous" behaviour, non-quadratic yield formulations were developed for anisotropic materials. Hill himself improved his criterion and proposed a non-quadratic form called Hill90 [113], which requires the identification of five material parameters, four from uniaxial tensile tests and one from balanced biaxial tests. Although the anomalous behaviour is captured with this criterion, in some cases the predicted yield surfaces are different from those either experimentally determined or predicted with polycrystalline models.

Hosford [116] was the first to introduce a non-quadratic yield function for isotropic materials, based on crystal plasticity. Barlat and Lian [38] extended the Hosford's criterion to materials exhibiting planar anisotropy; they captured the influence of the shear stress and proposed the yield function f according to Eq. (8) known as the Barlat 1989 yield criterion:

$$f = a|k_1+k_2|^M + a|k_1-k_2|^M + (2-a)|2k_2|^M = 2\sigma_e^M \tag{8}$$

where M is an integer exponent related to the crystallographic structure of the material, while k_1 and k_2 have the expressions given in Eq. (9):

$$k_1 = \frac{\sigma_x + h\sigma_y}{2}; \quad k_2 = \left[\left(\frac{\sigma_x - h\sigma_y}{2}\right)^2 + p^2\tau_{xy}^2\right]^{1/2} \tag{9}$$

with a, h, and p material parameters. Even if the number of material parameters to be identified is limited, they do not have a clear physical meaning and, furthermore, the parameter p can be identified only through a numerical procedure.

More recently, new yield functions were introduced to describe the anisotropic behaviour of steels, aluminium and magnesium alloys in order to improve the fitting of the experimental results. These models are usually based on a large number of material parameters, which need to be identified through different types of tests.

Barlat proposed in 2003 the Barlat 2000 criterion, a new model particularized for plane stress conditions [37], where the linear transformation method was used to account for the anisotropy. The yield function was expressed by Eq. (10):

$$\phi = \phi'(\mathbf{X}') + \phi''(\mathbf{X}'') = 2\bar{\sigma}^a \tag{10}$$

where a is an exponent depending on the crystallographic structure of the sheet metal, X is the linearly transformed stress tensor from the deviatoric stress tensor, and ϕ' and ϕ'' are two isotropic yield functions. The Barlat 2000 yield criterion needs eight material parameters to be identified, namely the three uniaxial yield stresses and anisotropy coefficients at 0°, 45° and 90° with respect to the rolling direction, the biaxial yield stress, and the coefficient of biaxial anisotropy.

Barlat et al. [36] extended the Barlat 2000 model for the 3D case developing the 3D yield criterion called Barlat 2004-18p; this criterion uses 18 material parameters, which, to be identified, require expensive equipment, a huge experimental effort, and the need for crystal plasticity models to evaluate some parameters. Nevertheless, the implementation of the Barlat 2004-18p model in finite element codes has proven its capability to predict the occurrence of six and eight ears in cup drawing processes, and is one of the phenomenological models able to capture more than four ears.

To introduce orthotropy in the expression of an isotropic criterion, Cazacu and Barlat [55] proposed an alternative method based on the theory of the representation of tensor functions: the method was applied to extend the Drucker's isotropic yield criterion [72] to transverse isotropy and cubic symmetries. Experimental research has shown that for some hexagonal close packed alloys (e.g. titanium-based alloys) the yield surface is better described by fourth-order functions. As a consequence, in order to describe such behaviour, Cazacu et al. [56,57] proposed an isotropic yield function for which the degree of homogeneity is not fixed, and is further extended to an anisotropic formulation: the most significant advantage of this criterion consists in its capability to provide an accurate description of the tension–compression behaviour of these alloys. In 2000 a new formulation of the yield function, named BBC 2000, was developed [25], based on the Barlat and Lian model [38]. Subsequently, by adding weight coefficients to that model, Banabic and his co-workers developed more flexible yield criteria [24,28,29]. In [24] a new expression of the plane stress potential was proposed, named BBC 2003, which was implemented in a modified version called BBC 2005 into finite element commercial codes [27]. The equivalent stress in the BBC 2005 yield criterion is defined according to Eq. (11):

$$[a(\Lambda+\Gamma)^{2k} + a(\Lambda-\Gamma)^{2k} + b(\Lambda+\Psi)^{2k} = \bar{\sigma}] \tag{11}$$

where $k \in \Im^{\geq 1}$ and $a, b > 0$ are material parameters, while Γ, Λ and Ψ are functions that depend on the planar components of the stress tensor according to Eq. (12):

$$\begin{aligned} \Gamma &= L\sigma_{11} + M\sigma_{22} \\ \Lambda &= \sqrt{(N\sigma_{11} - P\sigma_{22})^2\sigma_{12}\sigma_{21}} \\ \Psi &= \sqrt{(Q\sigma_{11} - R\sigma_{22})^2\sigma_{12}\sigma_{21}} \end{aligned} \tag{12}$$

The identification procedure calculates the eight material parameters *a*, *b*, *L*, *M*, *N*, *P*, *Q* and *R* by forcing the constitutive equations associated to the yield criterion to reproduce the following experimental data: stresses and anisotropy coefficients in tension along the three directions, the balanced biaxial yield stress, and the biaxial anisotropy coefficient.

In order to enhance the flexibility of the BBC2005 yield criterion, Comsa and Banabic [64] proposed a new version of this model, called BBC2008, expressed as a finite series that can be expanded to retain more or less terms, depending on the available experimental data.

By using points of the flow locus directly determined from the different uniaxial and multi-axial experiments (pure shear point, uniaxial point, plain strain point and equi-biaxial point), Vegter [231,232] proposed the representation of the yield function with the help of Bezier's interpolation. The Vegter criterion requires the determination of three parameters for each reference point, and needs up to seventeen material parameters to describe the planar anisotropy. The most important advantage of this criterion is represented by its flexibility thanks to the large number of material parameters to be identified; on the other hand, a large number of experiments are required for its calibration.

2.2.2. The value and limits to yield criteria

Most of the yield criteria above cited are implemented in finite element codes devoted to numerical modelling of sheet metal forming. Nonetheless, the Hill48 yield criterion is still the most widely used in practice, thanks to its effectiveness in describing the behaviour of metal sheets having a weak anisotropy and to the reduced number of material parameters to be identified, which, in turn, have a direct physical meaning. On the other hand, the enhancement of the criterion complexity, which improves the fitting of the experimental data, results in an increased experimental effort for identifying the related material parameters, which, in turn, often lack physical meaning, especially if identified through numerical techniques. The need to perform diversified, often multi-axial, tests, together with inverse analysis techniques to identify the material parameters, can restrain the application of the more complex models to the scientific community, limiting their use in the industrial practice.

Furthermore, the extension of the anisotropic yield criteria that take into account the influence of other process parameters, such as the temperature and strain rate, requires the coupling with crystal plasticity models, and the consequent increase of the experimental effort to identify the material parameters.

2.3. Phenomenological modelling of forming limits

The manufacture of a sheet metal part into a desired shape without failure, represented by either fracture or excessive localized thinning, is one of the main objectives of a proper process design. The prediction of the sheet metal forming limits assumes primary importance, even if the material formability cannot be easily quantified since it depends on many interacting factors related to both the sheet metal under deformation and the applied process parameters [26]. The first attempt to predict the forming limits was the phenomenological approach based on the concept of Forming Limit Diagrams (FLDs). Besides that, other two phenomenological approaches can be identified, namely linear methods, which assume the metal sheet as homogeneous, and Fracture Mechanics (FM), in which the rate of equivalent plastic strain scaled by a certain stress state dependent function integrated through the loading history provides a damage indicator variable.

2.3.1. Forming Limit Diagrams

The Forming Limit Diagram (FLD) [12,91,102,134] is the most popular criterion for predicting failure in sheet forming operations. It indicates the combination of the major and minor strains ($\varepsilon_1 - \varepsilon_2$) that can be applied to a metal sheet without failure. In the ISO 12004 standard [121] the onset of localized necking is chosen as the sheet failure criterion. The strain domain covered by the FLD must replicate as close as possible the various strain states arising during industrial sheet forming operations: to achieve this, various strain paths are applied to the metal sheet, ranging from equi-biaxial tension ($\varepsilon_1 = \varepsilon_2$) to pure shear ($\varepsilon_1 = -2\varepsilon_2$). However, in general, the strain state corresponding to simple tension ($\varepsilon_1 = -0.5\varepsilon_2$ for isotropic metals) is not exceeded.

The approach based on FLDs to predict the sheet failure is still the most widespread, especially in industry, and is currently implemented in the finite element commercial codes devoted to sheet forming simulation, mainly thanks to its simplicity in application. However, it presents several drawbacks, which have pushed the development of alternative approaches for predicting the sheet failure. The FLDs depend on the sample thickness, fall short in the case of non-linear (or non-proportional) strain paths, which very often characterize the sheet forming processes as was observed in [92,93,143]. Moreover, small variations in the properties from coil to coil of the sheet metal can cause significant variations in the material formability.

2.3.2. Forming Limits Stress Diagram

The strain path dependent nature of the FLD causes the method to become ineffective in the analysis of complex forming processes, especially multi-step forming. To make the strain-based FLD independent from the applied strain path, the concept of Forming Limit Stress Diagram (FLSD) was first introduced by Arrieux [10], and subsequently developed by Stoughton [211] (Fig. 3). Since the stresses cannot be directly measured, the procedure involved in drawing a FLSD comprises the experimental evaluation of a FLD, and the calculation of the corresponding stress values by using either the plastic flow rule or the finite element method. A combined experimental and theoretical methodology, based on the stress based forming limits, was proposed in [159], where it was demonstrated that the proposed strategy improved the formability predictions in multi-stage forming operations carried out with successive annealing stages to enhance the sheet metal formability. However, even if some researches show that the strain path does not affect the FLSDs (as examples, refer to [170,245,250]), their path independency is still questionable for complex combined loading paths, as pointed out in [244].

A successful attempt to predict the sheet failure subjected to a two-step forming operation by using the FLD together with a meta-modelling technique is described in [235], which requires a reduced experimental effort.

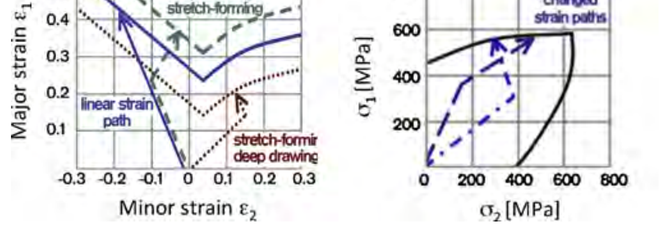

Fig. 3. From a path-dependent FLD to a non-path dependent FLSD. Adapted from [211].

2.3.3. Fracture Forming Limit Diagram

The FLD itself does not necessarily indicate whether the sheet failure occurs by local necking or fracture, even if it is the development of necks that effectively limits the part quality (for instance for visible panels in cars) rather than the occurrence of fracture. However, under some circumstances (e.g. deep drawn and stretched parts with complex geometries, where high strain gradients occur), it is the fracture that is likely to limit the attainable deformation [17]. In [75], the concept of fracture maps for metal sheets was first introduced, pointing out that the flow localization and fracture are given by two curves, which are represented on the same principal strain space. The plot of the major and minor strains at the point of the sample through thickness fracture in the principal strain space constitutes the Fracture Forming Limit Diagram (FFLD), where the principal major strain is calculated by using the incompressibility condition from the measurement of the sample thickness at fracture. A line sloping down from the left to the right represents the FFLD: as a first approximation, the line is at 45° in the principal strain space, and its intercept with the major strain axis is a material property, often called the workability index [186]. If the FFLD is well above the FLD, it may be assumed that fracture does not influence the sheet limit strains. The latter is the case of most ductile metals, whereas for more complex microstructure metals or peculiar process conditions, the necking is suppressed, therefore forcing the implementation of the FFLD.

In [186], the link between FFLD and fracture toughness was investigated, proving that the fracture strains along different biaxial paths may be predicted from the fracture toughness alone. The fracture toughness can be evaluated by using double edge notched tensile specimens according to the procedure presented in [18], where, by identifying the sheet metal properties from tensile tests and the fracture toughness, the effective strain at fracture was determined and decomposed into the in-plane fracture strains.

2.3.4. Linear methods

Methods based on linear analysis can give explicit solutions for predicting limit strains, and are generally easy to be applied. In the early 50s, Swift [212] developed a criterion for predicting the critical major strain for diffuse necking as a function of the strain hardening exponent and the strain ratio. Swift's analysis can be applied to any deformation condition, even if the predicted values in the range of negative strains are underestimated. However, since the necking typically arising in sheet forming is a localized one, Swift's analysis has a limited applicability. One of the first theoretical studies on localized necking was put forward by Hill [112], who introduced the bifurcation method joint with the flow theory; this method handles the onset of localized necking as a bifurcation from a homogeneous strain field to a highly localized deformation mode, and predicts the critical major strain for localized necking in the negative strain domain. Storen and Rice [210] incorporated the theory of plasticity into the classical bifurcation analysis to predict the localized necking over the entire range of the major-minor strains, and postulated that localized necking is due to the development of a corner on the yield surface. The method has limited applicability for negative strain ratios and reasonable results can be obtained for strain rate insensitive materials for positive strain ratios. The theory proposed by Storen and Rice was further developed to take into account the strain rate sensitivity, the influence of the sheet loading-unloading, and the effect of various yield criteria [189].

2.3.5. Fracture mechanics

Models based on Fracture Mechanics (FM) can be further subdivided into fracture criteria and void-growth-based models. Among the former, the most widely used models are those of Cockcroft and Latham [63], Brozzo [48], Oyane [191], and Johnson and Cook [128], whose formulations derive from energy considerations by assuming the deforming material as porous-free. Within the second category, McClintock [171] and Rice and Tracey [202] criteria are the most representative ones: they are based on analytical formulations devising isolated unit cells with voids under remote stress and strain fields. Models based on FM generally have a formulation that predicts the fracture occurrence when a damage indicator variable reaches a critical value. Although the damage accumulation is history-dependent, the damage variable is not coupled to deformation, and the yield function is not modified as the damage evolves, so it does not reflect any associated softening mechanism. However, their straightforward implementation into finite element codes as well as their intrinsic easiness in calibration favours their wide utilization.

More advanced fracture criteria have been recently proposed that take into account both the triaxiality ratio (defined as the hydrostatic pressure divided by the von Mises equivalent stress) and the shear stress state dependence by using the Lode Parameter or the third invariant (J_3) of the deviatoric stress tensor S ($J_3 = \det(S)$). Such models can give a more accurate failure prediction for complex stress states. Some examples can be found in [32,33,173], and in [161], where a modification of the Mohr–Coulomb fracture criterion is proposed. These recent models are superior to the ones above described, since they supply transferability of the material parameters for different stress states; however, their main drawback is represented by a major experimental effort since an increased number of characterization tests are required to identify the material parameters. As an example, Fig. 4 shows the numerical prediction of the strain field in a deep-drawn square cup, compared with the conventional Forming Limit Diagram (FLD) and the Modified Mohr–Coulomb (MMC) fracture criterion [161]: the former implies a safe condition at the cup corner, whereas the latter predicts the actual fracture occurrence with a good accuracy.

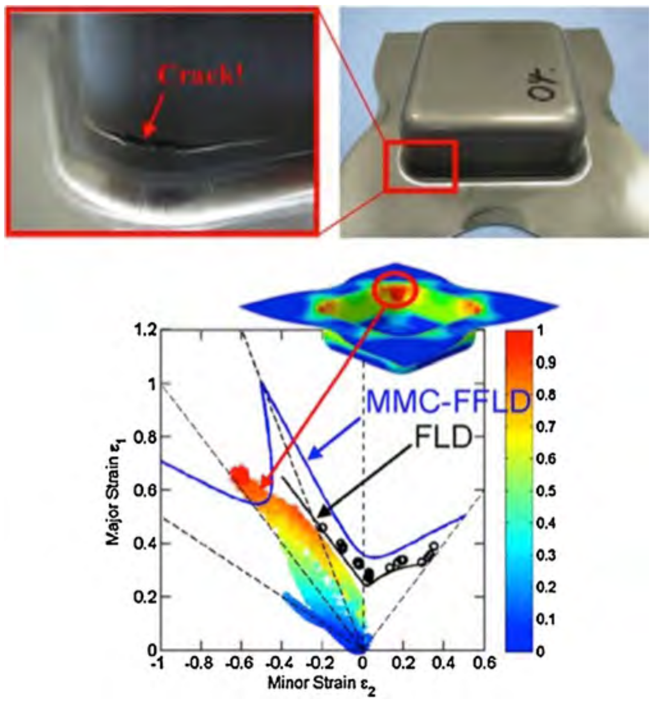

Fig. 4. Strain field in a deep-drawn square cup made in HCT690T steel compared with the Forming Limit Diagram (FLD) and the modified Mohr–Coulomb fracture model, and location of the crack.
Adapted from [161].

2.3.6. The value and limits to phenomenological modelling of forming limits

FLDs are the most widely used method of evaluating forming limits, especially at the industrial level. They provide a direct and intuitive evaluation of the limit strains leading up to the sheet failure, even if the dependence on the loading history and material anisotropy reduces their predictive capability, unless a huge experimental effort is provided. Even if FLSDs and FFLDs, have proved their ability to overcome some of the main drawbacks of FLDs, they are still restricted in use, even at research level. This is due to the need to be combined to numerical methods for the former and the suitability to peculiar cases for the latter.

While linear methods offer a reduced application in practice, due to the strong assumptions they are based on, FM-based models are increasingly applied in numerical simulation tools, thanks to their easiness in implementation and calibration through uniaxial mechanical tests. On the other hand, the need to predict the sheet metal forming limits under any state of stress is currently pushing the development of FM-based models that require more extensive calibration through multi-axial tests.

2.4. Physical modelling of forming limits

Marciniak and Kuczinski [168] were the first to propose a physical approach in modelling sheet metal forming limits, by introducing the idea of flow localization in a presence of a defect in the metal sheet. Other physical approaches have been recently proposed and are currently under development: they describe the material flow localization, eventually evolving into fracture, based on the evolution of the material damaging during forming. From the microstructural point of view, sources of strain localization into deformation bands, which will later on result in sheet fracture, can be regarded as a consequence of the strain hardening path dependence and softening mechanisms [11]. The former is caused by the destabilizing effects of a reduction in material stiffness due to the existence of a vertex or a sharp curvature at the loading point of the yield surface [11]. The latter may be due to the influence of the temperature on the material properties [158], or to the progressive deterioration of the material as a consequence of the occurrence of void-associated mechanisms, namely nucleation, growth and coalescence of micro-voids [189,227,241].

Physical models devoted to the prediction of sheet metal forming limits can be classified into: (i) non-linear methods based on the Marciniak–Kuczinki method, (ii) Micromechanical Damage Models (MDM), based on porous plasticity models, (iii) and Continuum Damage Mechanics (CDM) models, which modify the yield function as the deformation and damage progress.

2.4.1. Marciniak–Kuczinski method

The method proposed by Marciniak and Kuczynski [168] is based on the assumption that a necking gradually develops in a sheet from zones characterized by initial weakness, imperfection or inhomogeneity. The M–K model introduces a local imperfection in the sheet with uniform mechanical properties. The defect is inclined compared to the direction of the principal minor stress, and has to simulate the behaviour of a pre-existing defect. The M–K method predicts that the limiting strains are achieved when the ratio between the plastic strain increment inside the groove and the one outside reaches a critical value, corresponding to local instability. The predicted limit strains are in general overestimated in the domain of biaxial stretching and underestimated under plane strain conditions. The original M–K model was based on a sheet metal characterized by planar isotropy, the Hill48 yield criterion, the associated flow rule, and the power-law hardening law. Several authors have recognized that the shape and position of the predicted limit strains are strongly influenced by the chosen yield criterion and constitutive law implemented in the M–K model, and have proposed various modifications of it, thereby increasing the predictive capabilities of the method. A review about recent developments is proposed in [23].

2.4.2. Micromechanical Damage Models

Micromechanical based Damage Models (MDM) include porous plasticity models where the physical void volume fraction constitutes the primary damage variable. The irreversible plastic dilatancy is carried out using a hydrostatic stress dependent yield function together with the normality rule. Damage evolution is monitored through the void mechanism characteristic stages, namely nucleation, growth and coalescence of voids where the increase in the porosity results in the shrinkage of the yield locus and eventual softening. The Rousselier model [203] and the Gurson model [99], later modified by Tvergaard and Needleman [228] into the GTN model, are the most well known examples of micromechanical damage models. However, due to their hydrostatic stress dependent structure, they cannot predict failure mechanisms dominated by shear, where void distortion and void interaction, such as inter-void linkage with material rotation under shear, prevail. To overcome this limitation, the classical Gurson model was enhanced to take into account softening and localization under shear dominated stress states [187]. Applications of these models can be found in [78,197,209]. As an example, Fig. 5 shows the satisfactory agreement between the crack pattern experimentally observed in bending DP100 sheets and the one obtained from a numerical simulation carried out by using the shear-enhanced Gurson model. Further enhancements of the Gurson model to reflect the void shape dependency on the damage evolution were proposed in [89] and in [192].

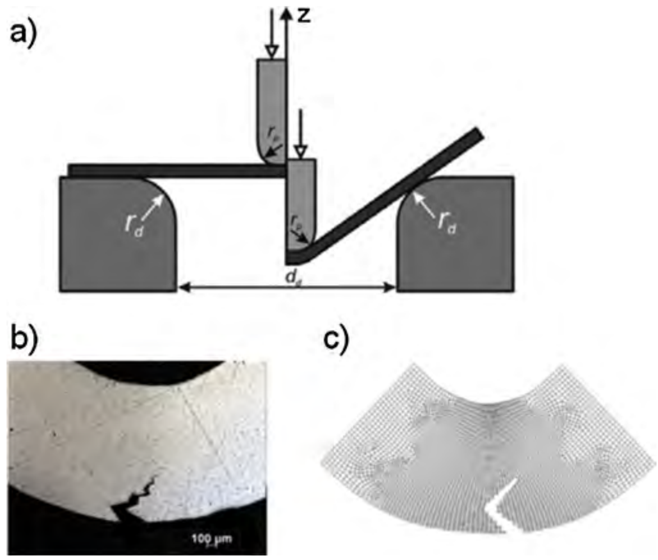

Fig. 5. Modelling of cracks when bending DP1000 steel sheets by using the shear-enhanced Gurson model: (a) experimental setup; (b) crack pattern experimentally observed in the bent section; and (c) numerical simulation result.
Adapted from [209].

2.4.3. Continuum Damage Mechanics

Continuum Damage Mechanics (CDM) is based on the effective stress σ_{eff} concept, first proposed in [130] and in [196], according to Eq. (13):

$$\sigma_{eff} = \frac{\sigma}{1 - D} \tag{13}$$

where σ is the material nominal stress, and D the material damage variable.

In this framework, the Lemaitre model [155], the most widely known and used, is consistently derived from thermodynamics concepts, where the evolution of the material damage modifies the material strain behaviour only through the effective stress, and the flow behaviour of the damaged material is modelled through constitutive equations for the undamaged material by replacing the nominal stress with the effective one. The irreversible microstructural weakening of the material due to the evolution of damage is modelled by coupling the deformation with an internal damage variable, which is introduced in terms of zero to high order tensors. The models based on the CDM can take into account both the shrinkage of the yield locus and the elastic stiffness degradation due to material deterioration, leading to elastic softening that can be effective in unloading regimes of the damaged materials.

In the Lemaitre model, the scalar damage variable D represents the extent of material deterioration due to isotropic damage, with areal density of defects at the plane of interest. The assumption of isotropic damage refers to a statistically and homogeneously distributed, shaped and oriented micro-void cluster. However, especially as regards non-proportional loading or anisotropic material behaviour, the evolution of anisotropic damage needs to be modelled: to do that, the scalar damage variable D has to be replaced by the second order damage tensor as presented in [50,149,156,157,174]. A further improvement is presented in [51] and in [236], where non-local effects were taken into account to bridge the gap between the micromechanical level and the classical continuum level, thanks to the incorporation of intrinsic material length parameters into the constitutive model.

2.4.4. The value and limits to physical modelling of forming limits

Physical models based on the M–K theory represent a versatile tool, show higher predictive capability, compared to phenomenological models, and generally imply a more reduced experimental effort compared to FLDs. However, the improvement of their prediction accuracy involves the use of more advanced yield criteria and hardening models, which, in turn, require dedicated testing and procedures for identifying the material parameters.

On the other hand, on the basis of consolidated experience in the field of bulk forming, MDM and CDM-based models are being increasingly applied for the prediction of sheet metal failure. Their description of the physical phenomena leading to material damaging, even if with different degree of abstraction, enables a high degree of accuracy, consistency and transferability of their prediction. The identification of the material parameters of MDM and CDM models requires mechanical tests, sometimes multi-axial, to account for the sheet anisotropic behaviour as well as advanced microstructural observations, coupled with inverse analysis identification techniques. Their use can be considered as being still limited to academic studies, but the potentialities they offer make them suitable for a more pervasive application, especially in the case of new categories of sheet materials and emerging forming processes.

2.5. Modelling of phase transformation and microstructural evolution

In the last two decades, new categories of high strength sheet metals have been introduced to the market to meet the increasingly stringent requirements for products characterized by a high ratio between strength and mass. Fig. 6 shows the mechanical characteristics of the new generation of High-Strength Steels (HSS) and Advanced High-Strength Steels (AHSS). These metals can be deformed either at room temperature or at elevated temperature; in both cases, their microstructure may evolve during and after straining, leading to phase transformation and/or to change in morphology of the microstructural constituents, which, in turn, greatly affect the mechanical and technological properties of the formed product. As a consequence, the modelling of the microstructural evolution of the sheet metal during straining is of primary importance to predict not only the sheet metal behaviour and formability during the forming process, but also the part characteristics during its service life.

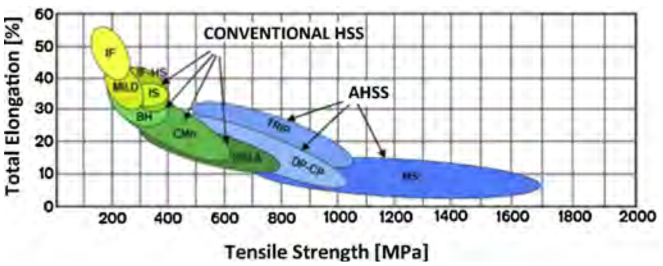

Fig. 6. Mechanical characteristics of High-Strength Steels (HSS) and Advanced High-Strength Steels (AHSS).

2.5.1. Modelling of phase transformation

Two main types of phase transformations may occur in metals, namely diffusional transformations, in which the new phase has a different chemical composition compared to the parent phase, and diffusionless or displacive transformations, which are characterized by no change in the parent phase chemical composition, but only in the crystal structure. The former kinetics usually follows a characteristic S-shape curve, modelled through the Avrami equation [19,20]. The Koistinen–Marburger equation [140] is applied to the martensite diffusionless transformation, evaluating the volume fraction of residual austenite as a function of temperature below martensite start temperature. The law of mixtures [141] is the easiest way to evaluate metal hardening, which accounts for the behaviour of the different phases that may arise during straining as a function of their volume fraction. In [106], the hardening law is applied to TRIP steels, where the material hardening is expressed as a function of the temperature, strain rate, and martensite transformation rate, taking into account the phase transformation thermal history.

If a phase transformation occurs under an applied external stress, the increased plasticity during the phase change is called transformation plasticity [151]. The modelling of the material behaviour passes through the accurate estimation of the total strain rate $\dot{\varepsilon}_{ij}$ increment given by Eq. (14):

$$\dot{\varepsilon}_{ij} = \dot{\varepsilon}_{ij}^{el} + \dot{\varepsilon}_{ij}^{pl} + \dot{\varepsilon}_{ij}^{th} + \dot{\varepsilon}_{ij}^{tr} + \dot{\varepsilon}_{ij}^{tp} \tag{14}$$

where $\dot{\varepsilon}_{ij}^{tp}$ is the transformation plasticity strain, and the terms of Eq. (14) are the elastic, plastic, thermal and isotropic transformation strain, respectively.

Two mechanisms are usually put forward to explain transformation plasticity, namely the Greenwood–Johnson's mechanism [94], and the Magee's mechanism [165]. Greenwood and Johnson associated the transformation plasticity strain with the micro-deformations of the weaker phase due to the volume difference between the product and the parent phases (accommodation or Greenwood–Johnson effect). Without applied stress, the average micro-plasticity is generally nil, whereas, when a deviatoric stress is applied, micro-plasticity will be canalized by the direction of the applied stress that generates transformation plasticity [214]. According to Magee, the transformation plasticity arises with the alignment of the newly formed phase having a preferred orientation in relation to the applied stress (orientation or Magee effect). If no external stress is applied, the orientation of the product phase is random, which makes the resultant of the microscopic stresses almost nil. The Magee's mechanism is particularly relevant in steels where the austenite transforms to martensite. It has been recently demonstrated that the loading history can affect the transformation plasticity [215].

Three categories of models can be currently identified to describe the transformation-induced plasticity, namely phenomenological models, micro-scale models, and multi-scale models. The phenomenological models can predict the material behaviour of metals showing transformation-induced plasticity by accounting for the effect of both macroscopic and microscopic parameters, based on experimental observations. The micro-scale models attempt to give a physical modelling of the phase transformation, whereas the multi-scale models reproduce the relevant micro-structural features, which are then scaled to a coarser level through homogenization techniques.

In [152] a micro-mechanical model is derived based on the determination of the plastic strain induced in a spherical parent phase by the growth of a spherical product phase core, neglecting the influence of the Magee's mechanism. In [223] a phenomenological thermally-coupled model for TRIP steels was introduced, and further improved to include the dependence from the stress state, temperature, pre-strain, and austenite grain size [124]. The first micro-scale model was proposed in [201], where a coupled approach based on experimental and numerical techniques was used to model the strain-induced martensitic transformation of austenite precipitates in a copper matrix. The microstructure was modelled through the Representative Volume Element (RVE) based on the unit cell approach. In [82], it was proposed to replace the plastic strain increment and the TRIP strain increment with an extended plastic strain that can account for both the Greenwood–Johnson and the Magee mechanisms. An example of a multi-scale model is proposed in [124], where the martensite inhomogeneity in a TRIP steel was taken into account in the meso-model of an austenite unit cell with martensite particle growing inside. A microstructural approach based on RVE was used in [229] to predict damage and failure in multiphase steels: the RVE made it possible to establish a correlation between the multiphase microstructure and the macroscopic failure behaviour. The micromechanical GTN damage model [228] was used in the RVE simulation. A 2D RVD is shown in Fig. 7 on the right, generated on the basis of the real micrograph on the left.

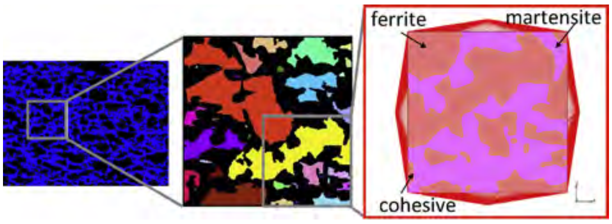

Fig. 7. Example of a 2D Representative Volume Element (RVE) based on microstructural observations [229].

2.5.2. Modelling of microstructural evolution

The recent introduction of sheet metal forming processes conducted at elevated temperature has required the application of microstructural models accounting for the evolution of the microstructural features during and after deformation in order to determine the post-forming product properties. A number of studies have addressed this topic to account for the evolution of microstructural features such as recrystallization, grain growth and cavitation [1,35,136,188,222]. In order to integrate microstructural deformation mechanisms into macroscopic continuum models, investigations have focused on building microstructure-based constitutive models by combining mechanical parameters with microstructural ones. Based on experimental observations of induced anisotropy and transient behaviour associated with internal stresses in superplastic deformation, a generalized multi-axial constitutive framework with internal variables was developed for superplastic forming processes [136]. The generalized framework was then extended to account for microstructural evolution including grain growth and cavitation during superplastic forming of lightweight alloys [1,126], and to develop multi-scale optimization schemes using microstructure-based failure criteria [188,222].

Among the various microstructural features, grain growth has been extensively studied and modelled due to its significant influence on deformation, especially at high temperatures and low strain rates. Grain growth models devoted to superplastic forming were proposed in [1,52,222], which were based on two independent grain growth mechanisms, namely static grain growth and deformation-enhanced dynamic grain growth. As an example, Fig. 8 shows the dynamic grain growth of AZ31 alloy at 400 °C and a strain rate of 10^{-4} s^{-1} [1]. The grain growth was successfully modelled using a linear function of the strain that can be easily incorporated in the constitutive relations.

2.5.3. The value and limits to microstructural models

Phenomenological models for predicting the evolution of microstructural features generally show a good predictive capability but require extensive experimentation to identify the material parameters. On the other hand, microstructural models based on micro- and multi-scale approaches, although showing a wider range of validity and better versatility, are currently limited in their use, especially in industrial practise, due to the complex combined experimental-numerical techniques needed for the identification of their material parameters.

Nonetheless, incorporating microstructural evolution models with the constitutive relations describing the deformation behaviour is essential for the accurate simulation of sheet metal forming processes conducted at elevated temperatures and involving large deformation.

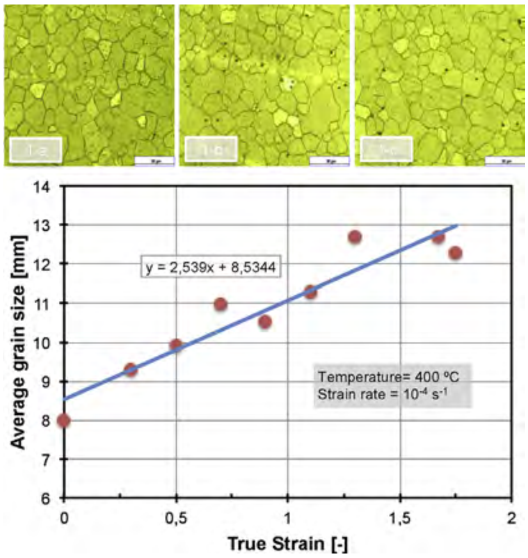

Fig. 8. (1) Grain structure of AZ31 alloy samples after straining at 10^{-4} s^{-1} and 400 °C to different strains (a) 0.3, (b) 0.7, (c) 1.1. (2) Linear relationship of dynamic grain growth vs. true strain at 400 °C [1].

3. Testing dedicated to sheet metals

A large variety of tests are available to describe the sheet metal behaviour, characterized by different levels of abstraction, from material testing-type to physical simulation experiments, which aim at reproducing the process operating conditions more closely. The data collected from these tests provide the basis for the identification of the material parameters of the models described in Section 2. These tests are classified here into four main categories, namely (i) uniaxial tests, (ii) multi-axial tests, (iii) cyclic tests, and (iv) tests dedicated to the determination of the sheet metal formability limits. The four categories will be reviewed in this section focusing on the conventional testing procedures, most of which are already standardized, as well as on the more innovative aspects in terms of equipment, data analysis procedures, and effects of process conditions.

3.1. Uniaxial testing

The paragraph reviews the category of tests carried out under uniaxial and monotonic loading conditions, namely uniaxial and layer compression tests. Uniaxial testing at elevated temperature and high strain rate is also reviewed.

3.1.1. Uniaxial tensile test

The uniaxial tensile test according to the ASTM E8 standard [16] is still nowadays the most widely used testing method for determining the sheet metal behaviour, mainly thanks to its intrinsic simplicity of execution. By using specimens machined at 0°, 45° and 90° with respect to the rolling direction, the yield stress and the anisotropy coefficients along the three directions can be evaluated, providing the basis for the calibration of most of the anisotropic yield criteria and hardening models.

Since a pure uniaxial stress state can only be obtained at uniform elongation, the maximum plastic deformation reachable by using conventional measuring techniques is rather low (usually in a range between 0.1 and 0.3). The use of optical strain measurement methods, such as Digital Correlation Technique (DIC), has partly overcome this drawback, allowing the direct and accurate strain measurement until fracture. Until necking, the state of stress in tensile tests is uniaxial, whereas most of the sheet forming processes are characterized by a biaxial state of stress, making the flow stress determined from a uniaxial tensile test insufficient to completely describe the behaviour of a metal sheet subjected to complex forming processes.

The evaluation of the sheet metal behaviour when subjected to micro forming processes or in real part cut-outs with small dimensions, where not enough material is available for the extraction of standard tensile test specimens, requires the use of mini tensile test samples, e.g. with a geometry designed according to the aviation standard LN 29512 [162], or with measuring areas even smaller than 1 mm^2 [205]. However, when using these miniaturized specimens, size effects have to be analyzed and need to be taken into account [207].

3.1.2. Layer compression test

Pawelski [193] was the first to propose the layer compression test, adapted from the standard compression test described in [68]. In the layer compression test, a stack of round blanks is compressed between two coplanar tool panels [69]: the uniaxial pressure loading leads to an equi-biaxial tensile load in the layered and compressed specimen. Investigations presented in [87] showed a good reproducibility by recording flow curves at values of strain up to 0.7, higher than those obtainable in uniaxial tensile tests. By additionally applying two 3D optical strain measurement systems perpendicular to each other, it is possible to locally investigate the time dependent anisotropic material behaviour [178] (see Fig. 9). In [6] the layer compression test was fundamentally revised and its results compared to those from compression tests carried out on bulk specimens of the same material in order to highlight its capabilities.

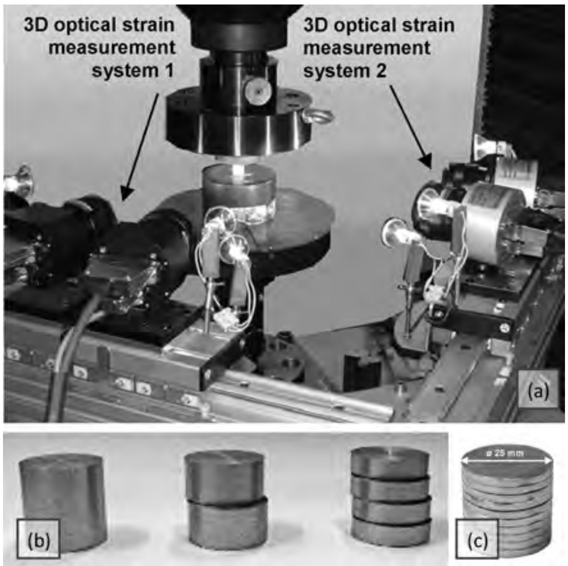

Fig. 9. (a) Experimental setup with two 3D optical strain measurement systems [178], and (b–c) specimens used for layer compression tests in [6] and in [178].

The obtainable flow curve from a layer compression test is greatly influenced by the quality of the force measurements as well as by the overall frictional conditions at the contact interface between the specimen and the tool plates. Therefore, a frictionless contact between the specimen and the tools is fundamental to avoid a three-dimensional stress state, thus, for instance, the use of Teflon foils is recommended. Furthermore, the single plates must be all oriented along their rolling direction, and must be concentrically aligned.

3.1.3. Uniaxial tests at elevated temperature

Uniaxial tensile tests at elevated temperature are usually performed by heating up the sheet metal sample to the testing temperature and carrying out the test at nearly constant temperature and strain rate, in order to evaluate the material sensitivity to temperature and strain rate. In [194] tensile tests at high temperature were used to determine the flow curves of the magnesium alloy AZ31B, proving that a temperature equal to 225 °C activates the pyramid sliding planes that allow a significant formability increase [70].

An experimental setup for uniaxial tensile testing suitable for determining the flow stress of the quenchable boron steel 22MnB5 under hot stamping conditions is described in [226], with testing temperatures up to 900 °C and strain rates of up to 1 s^{-1}. A similar setup implemented in a Gleeble 1500™ thermo-mechanical simulator is shown in Fig. 10 as proposed in [180] to investigate the flow behaviour of the same boron steel, but making use of an Aramis™ system to detect the sample strain till fracture. By using the same setup and applying the characterization approach proposed in [181], the temperature, strain rate and cooling effects on the 22MnB5 flow stress were evaluated. In [182], a MTS™ testing setup was equipped with an induction heater and an Aramis™ system to carry out tensile tests at elevated temperature on 22MnB5 sheets, with the aim of evaluating also the sheet metal anisotropy: the planar anisotropy was shown to be almost equal to zero for all the testing conditions, whereas the average normal anisotropy depended on the temperature.

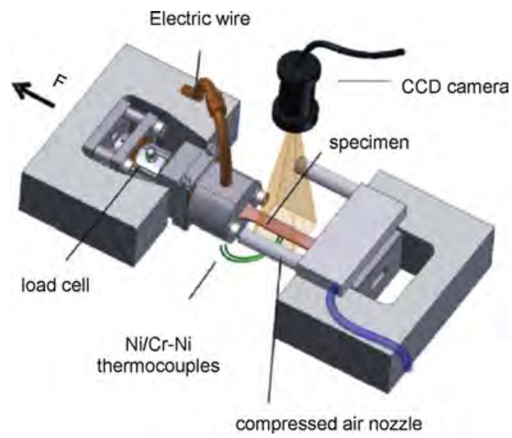

Fig. 10. Scheme of the Gleeble 1500™ modified chamber for testing sheets of 22MnB5 at elevated temperature [180].

3.1.4. Uniaxial tests at high strain rate

Besides the influence when forming at elevated temperatures, the strain rate has a major influence on the flow behaviour of sheet metals also when deforming in cold conditions in the high strain rate range. Emerging forming processes, such as electro-magnetic and impulse forming processes, are carried out under very high strain rate values, thereby addressing the need to evaluate the material behaviour under these conditions. Fig. 11 proposes a distinction between strain rate regimes, showing the range of strain rate where the inertia effects are relevant [80]. In [183] it was underlined that even the flow behaviour of conventional materials, like ultra-low carbon steels or interstitial free steels, can be sensitive to high values of the strain rate.

To evaluate the flow behaviour at intermediate strain rates, experimental setups, like drop towers and Split Hopkinson Pressure Bars (SHPBs), are widely used [80]. These testing setups are commonly individually designed and fitted to the investigated strain rate range and sheet metals. The SHPB usually presents the tensile configuration for testing sheet metal samples as shown in Fig. 12: as an example, this setup was used in [233] to investigate

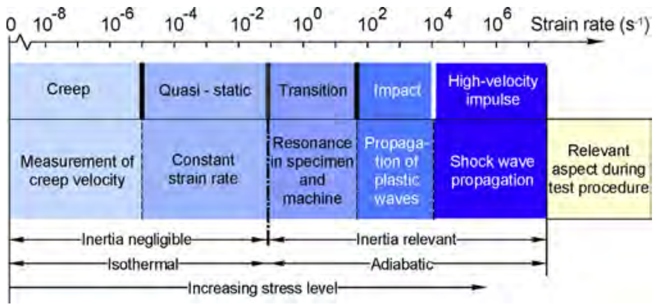

Fig. 11. Classification of the strain rate regimes, according to [80].

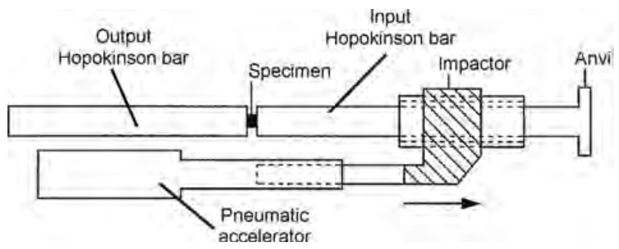

Fig. 12. Scheme of the Split Hopkinson Pressure Bar setup in the tensile testing mode [233].

the behaviour of different steels at strain rates between 1200 and 1800 s^{-1}.

When testing at high levels of strain rate, the sheet metal flow behaviour is completely different compared to the static one (see Fig. 13 for comparison): due to the high strain rate, the material first shows higher values of strength, which are subsequently reduced both by the continuously changing strain rate during the tensile test and, additionally, by the softening effects due to the heat generated in a nearly adiabatic system.

One of the major drawbacks of these experimental procedures that imply the conduction of tests at high strain rate or temperature is represented by the difficulty in keeping the strain rate and/or the temperature constant during the test itself. This leads to the difficulty in obtaining flow curves at constant strain rate and temperature to be later on used for the identification of the material parameters of the hardening laws and yielding criteria. To overcome this general problem of material characterization, the identification of the material parameters can be fulfilled through inverse analysis techniques that use the parameters measurable during the tests and either analytical or finite element-based models. However, the main limitation of inverse analysis techniques, represented by the risk of an ill-conditioned problem, has to be overcome by a suitable choice of the measured parameters.

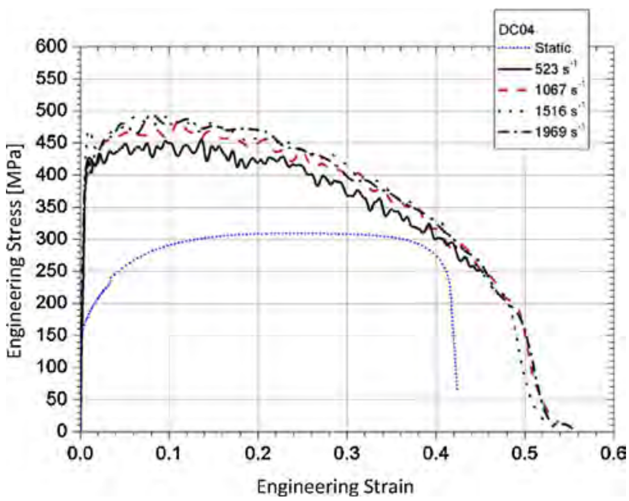

Fig. 13. Comparison between static and dynamic engineering stress–strain curves [233].

3.1.5. The benefits and limitations to uniaxial testing

The evaluation of the sheet metal behaviour under uniaxial and monotonic loading conditions is still the most widely used in the industrial practise, since it provides a quick tool for gaining material data, thanks to its simplicity of execution and direct understanding of the obtainable data. Most of the material parameters of the hardening laws and yield criteria today implemented in the finite element commercial packages have been identified through uniaxial tensile tests, which makes the results of most of the numerical simulations carried out nowadays dependent on the accuracy of these input parameters. Furthermore, uniaxial tests still represent the most used testing approach to evaluate the sheet metal behaviour at elevated temperature and high strain, as the increased complexity of the testing setup and data analysis due to temperature and strain rate can be still dealt with in a straightforward way.

3.2. Multi-axial testing

Within this context, tests under multi-axial and monotonic loading conditions are reviewed, namely bulge, biaxial tensile and shear tests. In addition, testing setups and procedures for testing at elevated temperature and high strain rate are also described.

3.2.1. Bulge tests

A testing setup suitable for the determination of the stress–strain curve under a biaxial stress state, which also neglects the influence of friction, is the hydraulic bulge test. This test, which uses both hydraulic equipment and optical strain measurement techniques, will be standardized in the ISO 16808 [122], currently under development.

The bulge test is a stretch-forming process, where the biaxial stress state occurs in the curved surface of the clamped specimen by exposing it to a hydraulic pressure usually exerted by water-based fluids [90,129,150]. As a result of clamping, the specimen thickness reduces until bursting. The flow stress of the sheet metal can be calculated on the basis of the measurement of the dome-shaped specimen, by using an analytical closed form solution and assuming that the sheet metal behaves like a thin membrane. Because of the difficulties in measuring accurately the dome geometrical characteristics, the flow curve is usually determined by using inverse analysis techniques applied to the numerical simulation of the test and by measuring only the fluid pressure and the dome height. 3D optical strain measurement systems can be also used to calculate the strain and radius of the specimen curvature, obtaining more accurate flow curves [96]. The maximum achievable values of strain are between 0.5 and 0.8, depending on the material. To obtain larger values of true strain, the use of lock beads was proposed in [96].

The main advantages of the hydraulic bulge test are represented by the simple specimen geometry consisting of a rotational symmetric blank, and the capacity to reach high values of true strain before the instability or the bursting occurs. However, in testing ductile materials, which do not fracture until a true strain of approximately one is reached, the bulge shape is not spherical towards the end of the test, and this forces to use numerical methods for the flow curve determination [97].

The Viscous Pressure Bulge test (VPB) is a variation of the hydraulic bulge test that uses a viscous medium to pressurize and deform the blank [100]. The same procedure as in the conventional hydraulic bulge test is used to determine the sheet metal flow curve. Similarly to the hydraulic bulge test, the VPB test can be also used to determine and compare the formability of different sheet metals [5].

The dome test is a variation of the Limiting Dome Height (LDH) test that uses nearly "perfect" lubrication conditions between the solid spherical punch and the sheet blank. As a result, the maximum thinning of the deforming sheet occurs at the apex of the dome. By measuring the punch force and displacement, and by using an inverse method based on numerical analysis, the biaxial stress–strain curve can be obtained. The dome test is often preferred in industry because it is simple to carry out and does not present the problem of oil leakage that may be encountered in the hydraulic bulge test. However, it is not easy to find a lubricant that can almost eliminate friction and makes it possible to obtain the maximum thinning of the sheet at the apex.

3.2.2. Biaxial tensile tests

The planar biaxial tensile test is a testing setup for determining the sheet metal behaviour as well as the yield locus in the first quadrant of the stress space. It is also useful to determine the coefficient of biaxial anisotropy, namely the ratio of the strains along and perpendicular to the rolling direction. The biaxial anisotropy coefficient describes the slope of the yield locus at the equi-biaxial stress state and is used for the calibration of various yield criteria. The standard ISO 16842 [123] devoted to biaxial tensile tests is currently under development.

The planar biaxial tensile test is usually carried out by stretching cruciform shaped specimens, where the relevant measuring zone of the biaxial stress state is in the middle of the specimen. Various researchers developed machines for biaxial testing as reviewed in [105] with a thorough analysis of the advantages and drawbacks of all the suggested concepts. The machines for biaxial testing mainly belong to two different categories: built-in fixtures for universal machines, as proposed in [46] or in [217], and stand-alone machines with self-contained control systems, as developed in [145] and in [176]. The machines for biaxial testing can be further classified as displacement-driven biaxial machines, such as the one shown in Fig. 14, and load-controlled biaxial machines, such as the one shown in Fig. 15. The former use symmetrical jointed-arm or cam mechanisms to apply in-plane biaxial loads to a cruciform specimen. The stroke is obtained with at least one actuator, but closed-loop controls are difficult to be realized due to the rigid geometrical configurations that cannot be varied during the test. When large deformations are applied to the specimen, the displacement-driven machines may suffer from kinematic incompatibilities, causing side bending of the specimen [79]. On the other hand, the use of four independent actuators represents the most reliable technique for obtaining well-defined biaxial states of stress and strain in the specimen central zone, even in the case of strong anisotropic material behaviour [41,166]. The actuators can be hydraulic, electromechanical or fully electrical, and the closed loop controls are obtained using multiple load cells per axis in order to supervise the symmetry of the loading conditions during the test and to avoid the application of shear loads to the specimen test region.

Extensive research studies are still devoted to the design of suitable cruciform geometries, usually by means of numerical simulations, with the aim of having most of the deformation at the specimen centre section and avoiding stress concentrations in other zones of the specimen. The premature failure at the specimen arms represents one of the major drawbacks that still limits the application of cruciform biaxial tensile tests: it can be avoided by adding radii between adjacent arms, and/or reducing the specimen thickness in its gauge section, thus causing the stress to concentrate and the gauge section itself to experience higher levels of plastic deformation. As examples, in [2,53,148,153,177] the specimen geometry was designed and optimized in order to get an approximately homogeneous strain distribution in the middle of the specimen. Numerical simulations of the specimen loading can also be useful to evaluate the stress field in the gauge zone on the basis of the applied loads, the transfer of the external loads to the internal stresses being one of the major concerns of planar biaxial tests for the subsequent calculation of plastic yielding. Another major issue is represented by the possibility of having an accurate strain measurement, preferably by using non-contact methods. However, even if an accurate measurement of the resulting strain is carried out, the achievable values of strains in planar biaxial tests are usually lower than the ones obtainable in the bulge tests above presented.

In 2013, an advanced biaxial cruciform testing system was built and demonstrated at the National Institute of Standards and Technology (NIST) Centre for Automotive Lightweighting in Gaithersburg, MD USA [239]. The system comprises many advanced measurement techniques in order to probe multi-axial mechanical behaviour, namely four independently controlled hydraulic actuators with real-time strain feedback control to allow forming under non-linear strain paths, 3D digital image correlation to measure strains, infrared camera for adiabatic heating (from −50 °C to 350 °C with a resolution of 0.01°, 50 frames/s at 1.4 M pixels) as well as in situ X-ray diffraction to directly measure stresses during testing. A scheme of the testing setup and an example of the sheet metal specimen clamped in the system are shown in Fig. 16. The real-time correlation between the

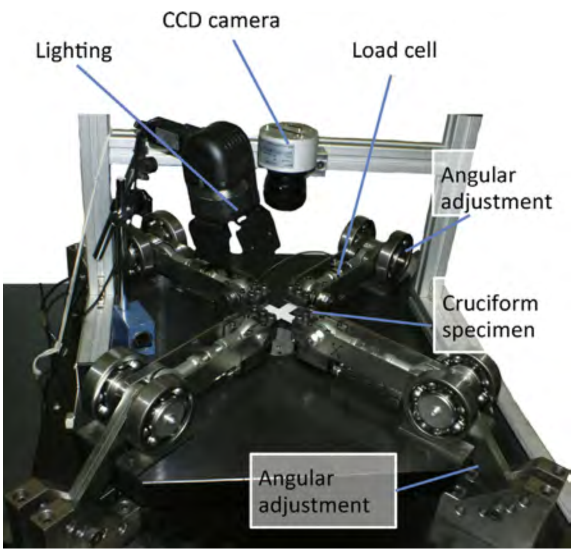

Fig. 14. Example of a displacement-driven biaxial testing setup [176].

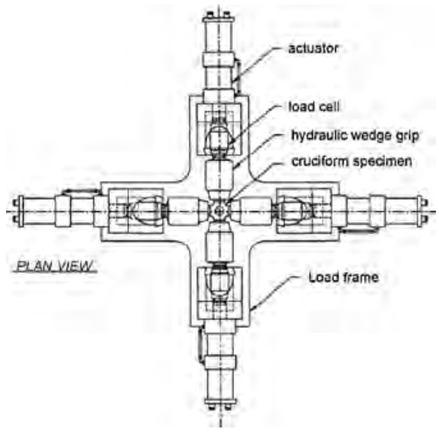

Fig. 15. Example of a load-controlled biaxial testing setup [166].

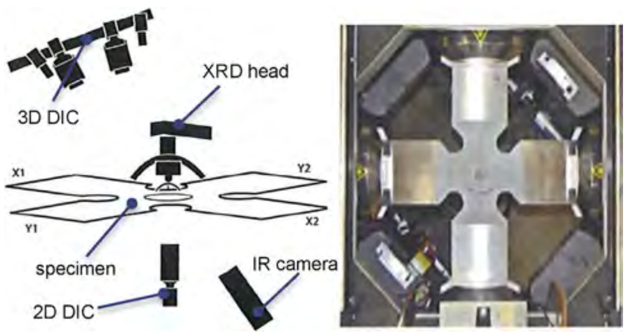

Fig. 16. Cruciform biaxial testing setup developed at NIST on the left, and sheet metal specimen clamped in the system on the right [239].

stress and strain measurements thanks to the implemented measuring techniques is expected to alleviate the need for the specimen geometry optimization.

3.2.3. Shear tests

In order to investigate the material behaviour at larger strains, a testing method for realizing simple shearing was first proposed by Tekkaya et al. [220] and later on by Miyauchi [185]. The simple shear test has the advantage of testing the material without necking or buckling, avoiding any frictional influence, and makes an easy determination of the stress–strain curves possible. The sample preparation according to the procedure presented in [185] consists in realizing the two shear zones shown in the specimen of Fig. 17(A), where the shear stress in the two bridges results from the in-plane displacement of the zone between the two bridges. In [199] the shear test was conducted on a clamped rectangular blank under monotonic and cyclic loading, and in [200] the anisotropic behaviour of a sheet metal subjected to simple shear was studied, by deforming specimens extracted from the blank at different orientations with respect to the rolling direction, corresponding to the equivalent anisotropic investigation through uniaxial tensile tests. In [22] a planar simple shear test is used to get more direct information on the material strain hardening response. A newer testing setup was proposed in [118] and illustrated in Fig. 17(B), where a shear fixture was mounted in a universal testing device following the recommendations reported in [185]. Efforts were made to analyze the homogeneity of shearing in the effective range and to evaluate different geometries of the shear bridge, by varying the sheet thickness, width and length.

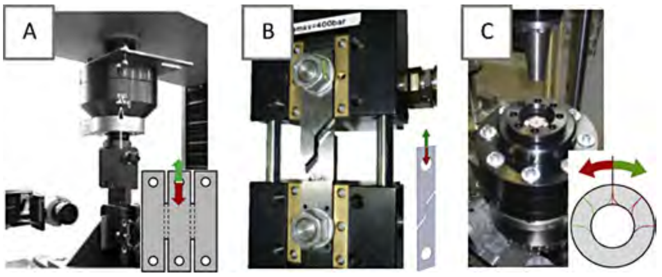

Fig. 17. Simple shear testing setup according to Miyauchi [185] (A), modified ASTM B831 testing setup according to [118] (B), and in-plane torsion testing setup according to [221] (C).

Another possibility of material testing under shear conditions is the in-plane torsion test, first recommended by Marciniak [167]. The specimen for this test, shown in Fig. 17(C) fixed in the testing setup, consists of a simple circular sheet metal blank clamped along the fringe and on the inner axis. The shear stress state is introduced by the torsion of the inner axis, which leads to a shear deformation in the free area of the specimen. Because of the linearity of the shear stress to the square radius, the highest value of shearing is reached at the inner clamp [167]. At increasing radial distances, the effective strain decreases. A method for determining the flow curve from the torque curve over the angle of rotation was developed in [221]. Here, the flow stress was determined without assuming any form for the flow curve, obtaining larger equivalent strains compared to the uniaxial tensile test. The operating window of the in-plane torsion test was given in [221] as a function of the sheet thickness and inner clamping radius (Fig. 18), covering also the process limit for buckling. In [39] the geometry of the specimen for the same test was optimized to decrease the tendency of buckling. In [47] an in-plane torsion test with a modified specimen for shear testing was introduced, consisting of two bridges and a defined shear zone: by using this geometry, the anisotropic behaviour can be evaluated, and thanks to the small area of shearing, relatively low clamping forces need to be applied.

Besides the conduction of the Miyauchi simple shear test with two shear bridges and the in-plane torsion test, another simple shear test method according to the ASTM B831 standard [13] is

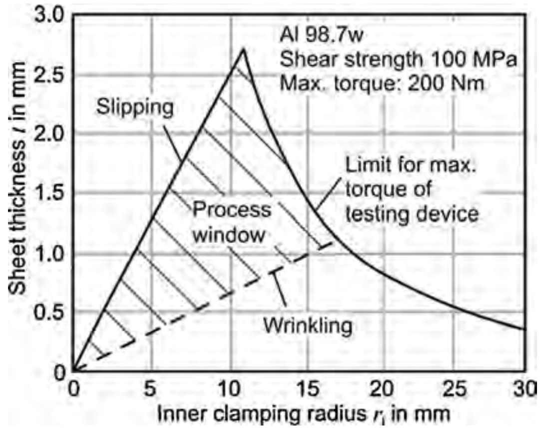

Fig. 18. Operating window of the in-plane torsion test [221].

used to analyze the material behaviour under shearing deformation: thanks to this method, a single shear test is proposed with only one effective range. By applying two notches on both sides of the shear zone, a modified ASTM simple shear test to investigate the constitutive behaviour of AA5754 at large strains was used in [131].

Since the strain distribution in shear tests is strongly dependent on the shape of the shear zone [8], the implementation of optical strain measurement systems has recently brought more accurate results. In [242] an experimental method (Fig. 19 upper part) based on the in-plane torsion test was proposed to determine the material flow curves using an optical strain measurement system, which made it possible to acquire levels of strain up to 1.0 (an example of the obtainable flow curves is shown in Fig. 19 lower part).

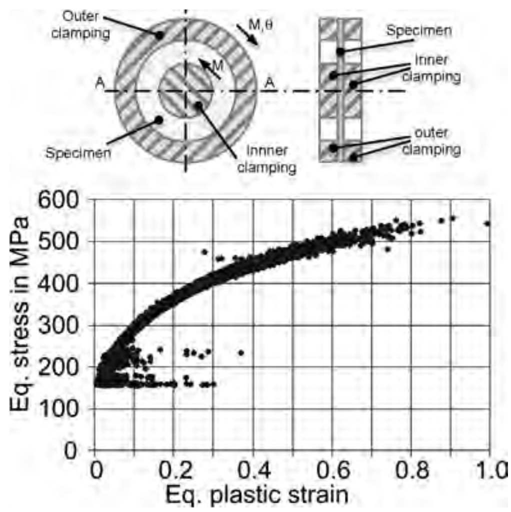

Fig. 19. Application of the in-plane torsion test to determine flow curves at high strain [242].

3.2.4. Multi-axial tests at elevated temperature

Hydraulic bulge tests were conducted at elevated temperature on sheets of the AZ31 magnesium alloy by using a submerged tool, designed to minimize the temperature variation in the sheet [133]. In [109] the influence of different strain rate values up to 0.1 s^{-1} and temperatures between 200 °C and 250 °C on the magnesium alloy behaviour was investigated by using a hydraulic bulge setup: it was shown that the temperature increase as well as different strain rate levels cause a significant variation of the yield stress of ±50%. A review of the effects of temperature and strain rate on the flow behaviour of aluminium–magnesium alloys can be found in [224], where the authors criticize the usual disregard given to the evaluation of the strain rate influence as well as the lack of flow properties under biaxial stress conditions at elevated temperatures. A testing setup, which combines the features of a bulge test and a deep-drawing test, was used in [95] under hydro-mechanical deep-drawing testing conditions to investigate the flow behaviour of aluminium alloys at elevated temperature.

In [177] a combined experimental–numerical approach is described, aimed at determining the yield stress of the magnesium alloy AZ31 under different biaxial stress conditions in the first quadrant of the yield locus at elevated temperature. Likewise, an experimental setup based on a tool for stretch drawing was developed in [85] in order to investigate the onset of yielding of aluminium and magnesium alloys at elevated temperature. In both these studies, the specimen geometry was optimized through finite element analysis. Due to unrestricted visual access, laser heating as well as optical measurement techniques were applied: Fig. 20 shows the developed experimental setup.

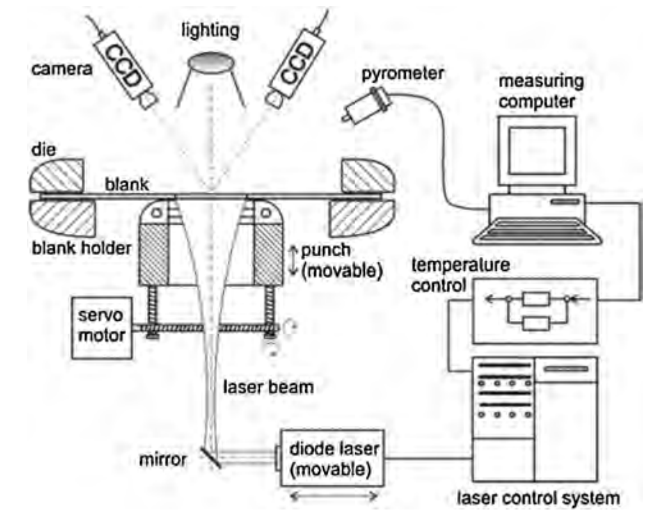

Fig. 20. Experimental setup to investigate the plastic yielding at elevated temperature [87].

An experimental setup for biaxial tensile testing at elevated temperature was also proposed in [88]: Fig. 21 shows some specimen designs with different geometrical features, such as notches at the edges to avoid early cracks, thickness reductions in order to enforce the straining in the centre, and slits to reduce the transversal stiffness of the arms.

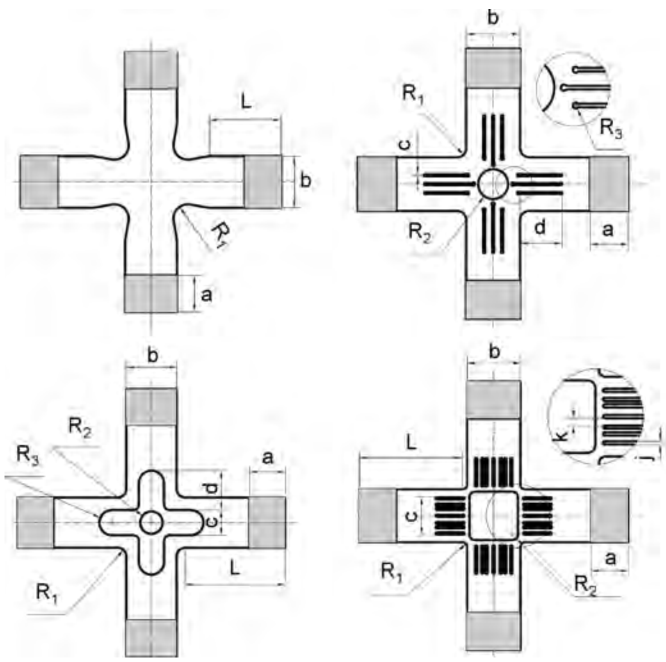

Fig. 21. Various cruciform specimen concepts with notches, thickness reductions and slits [88] for biaxial tensile testing at elevated temperature.

3.2.5. Multi-axial tests at high strain rate

To characterize the sheet metal behaviour at high strain rate, a hydraulic bulge test, adopting a rubber-pad as pressure carrying medium, was proposed in [198] and installed on a Split Hopkinson Pressure Bar bench. High speed punch stretching was conducted in [61] to determine the flow curves at high strain rates for electromagnetic forming processes. In [139] the electromagnetic forming process was used to identify the sheet metal yielding behaviour under very high strain rate conditions. In [98] the inverse method was applied to different experimental setups for determining the material parameters of the Barlat yield criterion. However, the set of material parameters identified by such method is only valid for the chosen model, and strongly depends on the assumptions of the model itself.

3.2.6. The benefits and limitations to multi-axial testing

The pervasive adoption of numerical modelling techniques in the design of sheet metal forming processes supported by more accurate models for predicting the sheet metal behaviour has instigated a strong demand for the development of multi-axial tests. Though uniaxial tests have proved invaluable for a quick determination of the material behaviour, the scientific community agrees that multi-axial responses are more applicable to represent the state of stress present during a sheet metal forming process, thereby causing the concept of material testing to evolve to the level of physical simulation experiments.

On the other hand, multi-axial tests are usually characterized by a higher degree of complexity compared to uniaxial tests, both in terms of testing machines and testing procedures to identify the required data, which still limit their effective application at industrial level. Inverse analysis techniques are often involved to identify the material parameters, which force the joint use of numerical and experimental techniques, increasing the analysis efforts.

3.3. Cyclic testing

The paragraph reviews the category of tests carried out under cyclic loading conditions, including both proportional and non-proportional loading, suitable for identifying the material parameters of the hardening models devoted to the description of the sheet metal behaviour under complex strain paths.

3.3.1. Tension–compression tests

The characterization of the Bauschinger effect and the identification of the material parameters of the kinematic hardening laws can be fulfilled through cyclic tests. Uniaxial tensile tests with inversion of the load direction are usually carried out, as recommended in [247]. However, the conventional procedure for conducting in-plane tension–compression tests has been recently reviewed to overcome their main limitations. To suppress the buckling that the sheet specimens are prone to exhibit during the in-plane compressive loading and the measurement of the specimen strain, the specimen surface can be covered with a support structure during testing. In [43] a normal pressure was applied to the specimen surface by means of plates moved by hydraulic actuators and the strains were concentrated only along the exposed side of the specimen. A comb-based device was used in [146] to maintain the normal contact during testing between a portion of the test specimen surface and the support structure, while the strains were measured using a conventional strain gauge over a region on the sheet surface that was unsupported by the comb-device (Fig. 22).

A wedge-shape device was also designed to measure tension–compression behaviour by adopting a geometry that allowed for full normal contact during testing. However, a modified specimen geometry was required in order to use fins on the exterior of the specimen for measuring the strain, increasing the achievable compression strain and eliminating at the same time the risk of buckling (Fig. 23 on the left) [54]. More recently, a transparent

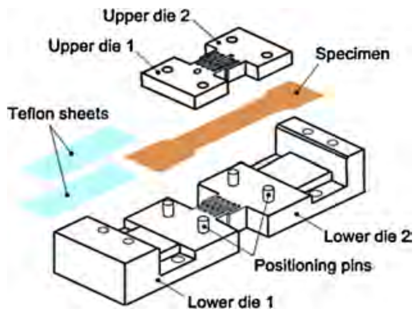

Fig. 22. Comb-device to investigate the sheet metal behaviour under tension-compression loading [146].

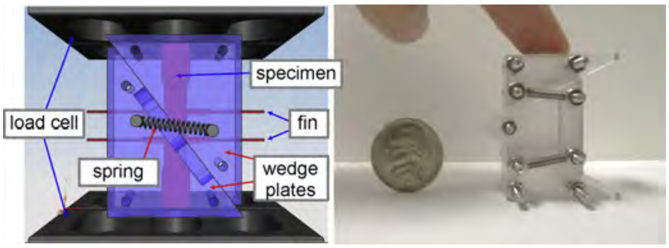

Fig. 23. Wedge-device to investigate the sheet metal behaviour under tension-compression loading using macro-scale samples [54] on the left, and using mini-scale samples for ultra-thin sheets on the right [164].

wedge-shape device was shown to be also suitable for tension–compression testing of conventional dog-bone shaped specimens, enabling optical strain measurement using digital image correlation in order to circumvent problems related to the strain measurement (Fig. 23 on the right) [164].

3.3.2. Other cyclic tests

Cyclic shear tests with a modification of the conventional specimen geometry were proposed in [175] and in [243], to evaluate the material behaviour under cyclic testing in shear stress conditions.

When testing high strength steels, the cyclic bending test was recommended in [248], where the sheet metal specimen was loaded perpendicularly to the plane. A new bending testing setup was developed in [71] for cyclic testing of high strength steels by load reversal: thanks to the inverse parameter identification method, it was shown that the cyclic bending test can represent a time and cost saving alternative for the evaluation of the Bauschinger effect. A cyclic bending test and a corresponding inverse method for identifying the material parameters were suggested in [86], whereas, for pure bending, a device was presented in [42]. Moreover, the three-point cyclic bending test and an inverse calculation method were used to identify the material parameters [249].

Orthogonal tests and tension–tension tests were introduced more recently to evaluate the kinematic and distortional hardening of metal sheets subjected to non-proportional strain paths, the former being characterized by two monotonic loading paths with perpendicular loading directions, usually plane tension followed by shear [190], the latter by tension–tension tests [101], namely two-steps loadings, the first in the rolling or transverse direction, then the second every 15° from the first loading axis.

3.3.3. The benefits and limitations to cyclic testing

Tensile-compression tests with load reversal are still the most widely used cyclic tests for evaluating the sheet metal behaviour upon load reversal, thanks to the easiness in extracting the stress–strain curve and identifying the material parameters of the kinematic hardening models. However, the increase in the complexity of hardening models to predict the material behaviour requires testing under complex strain paths, which needs not only dedicated testing equipment, but also sophisticated data analysis.

3.4. Formability testing

Formability tests can be basically divided into three main categories, namely intrinsic tests, simulative tests, and tests devoted to the determination of the Forming Limit Diagrams (FLDs) [218]. The main features of these three categories will be described in the following.

3.4.1. Intrinsic tests

The intrinsic tests provide comprehensive information about the basic mechanical properties of the sheet metals, which can be related to sheet metal formability characteristics independent of the sheet thickness and surface conditions. However, they reproduce strain states much simpler than that characteristic of the industrial processes, and completely rule out the effect of the processing variables.

The most widely used intrinsic test is the uniaxial tensile test [16], which applies a stress state typical of the drawing region under the blank-holder, where the minor strain is negative; its main advantages are represented by the easiness and rapidity in carrying out tests on universal testing machines and extracting data by following conventional procedures reported in dedicated standards, the absence of friction effects, the low scatter presented in the experimental results, and the chance to use optical devices for the strain measurement. The intrinsic formability parameters obtained through a tensile test and usually evaluated as a measure of the metal formability comprise the uniform and total elongation, the true strain at fracture, and the Lankford anisotropy coefficients. The strain hardening and the strain rate sensitivity exponents can be as well evaluated from the tensile test results; however, since they are obtained from a simple curve fitting, by usually assuming an exponential function, they are found to be constant, whereas for some alloys (such as advanced high strength steels) they vary with the strain. The evaluation of the material response in the plane-strain state can be fulfilled through the plane-strain tensile test [67], which ensures the minor strain component equal to zero, thanks to a modification of the sample geometry, by increasing its width and decreasing the gage length (sketch of the specimen in Fig. 24 on the left). The stress conditions of the biaxial stretching characteristic of the strain state in many stamping processes can be replicated through either a Marciniak biaxial stretching test or a hydraulic bulge test. The Marciniak biaxial stretching test [168] allows creating a uniform in-plane biaxial strain at the sample centre by using a cylindrical punch with a central hole to overcome the friction effect (sketch in Fig. 24 on the right). The obtained strains can be measured through markings applied on the sample, such as circles or squares.

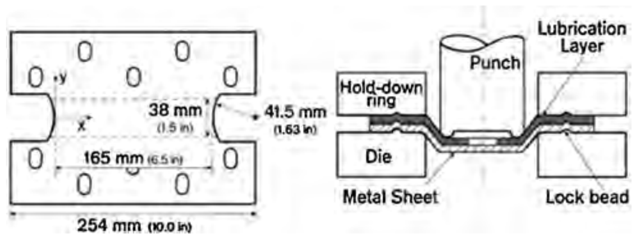

Fig. 24. Sketch of the plane-strain tensile specimen on the left [67], and sketch of the Marciniak biaxial stretching test on the right [168].

The hydraulic bulge test [73] allows biaxial stretching deformation of the sample into a dome by the action of a pressurized fluid, which involves out-of-plane stresses and strains in the blank. No friction is involved, as would be the case using a punch, and therefore the test reproduces pure biaxial stretching conditions. Since the level of strains attainable with the hydraulic bulge test is much higher than those achievable in tensile testing, and the biaxial stretching is a stress state commonly arising in stamping, the bulge test is sometimes used to simulate sheet forming operations.

3.4.2. Simulative tests

The *simulative tests* impose strain and stress states that closely reproduce the ones arising in a particular forming operation, and include the effects of parameters, such as friction, that are not taken into account in the intrinsic tests. They tend to be less reproducible compared to intrinsic tests and must be performed under carefully controlled testing conditions to minimize the results variability. Friction can significantly affect the results, which may differ depending on the adopted lubricant, therefore making this kind of tests less reproducible. The simulative tests are usually classified according to the forming operation they are aimed at reproducing, namely bending, stretching, drawing, and stretch-drawing.

The simple bending test [14] provides the minimum recommended inside radius of curvature to form a 180° bend in a sheet of specified thickness without failure. The test is repeated using a smaller and smaller bend radius until fracture in the sheet occurs. The stretch-bending test provides information about the material formability when subjected to combine bending and stretching, which happens when the sheet is forced to pull over a punch or die radius. The depth of punch indentation at the maximum force represents the typical output of the stretch-bending test.

The Erichsen test and the Olsen test [15] are cupping tests and were the first to be developed for estimating the sheet metal stretchability, namely the sheet metal formability under stretching conditions. Both the tests stretch the sheet over a hardened steel ball, and the height of the produced cup at failure is the measure of the material stretchability. They differ from the size of the tools, but they both suffer of results variability and poor reproducibility, mainly due to the small size of the involved tools, the difficulty in guaranteeing a stable lubrication and the possibility to have drawing. Moreover, the correlation with the strain hardening exponent was found to be not totally satisfactory. To overcome the drawback of the cited cupping tests, tests using larger diameter punch and draw beads to prevent draw-in were developed. Among them, the hemispherical dome test is the most widely used [110]; again, the depth of the punch indentation at the fracture onset generates the formability index. The limit dome height test [21] is another stretching test carried out with a large diameter hemispherical punch (dia. 100 mm) and draw beads in the die to prevent draw-in, specifically dedicated to the reproduction of plane stretching conditions (sketch in Fig. 25 on the left). Samples with different width samples are stretched over the punch and the height of the dome at fracture is measured. The height at which the dome fails shows a minimum at a critical sample width. This minimum height is known as the limiting dome-height near plane strain (LDHo) and is extensively used as a formability index especially in industry since more than 80% of the stamping failures occur when the strain state is close to plane strain conditions. The main drawback of this test lies in the difficulty in determining the critical sample width for a given sheet metal, due to the difficulty of reproducing stable plane strain conditions over large regions of the sheet sample. The OSUFT (the Ohio State University Formability Test) [237] was introduced to overcome the limit dome height test limitations, using a punch whose geometry was optimized by numerical simulation to guarantee plane strain conditions.

The most common test for evaluating the material drawability is the Swift cup test [212], which involves the drawing of circular samples of various diameters into cups by the action of a flat-bottomed cylindrical punch (sketch in Fig. 25 on the right). The formability index is in general defined as the Limiting Draw Ratio (LDR), namely the ratio between the sample maximum diameter drawn without tearing and the punch diameter. The Swift method is widespread, even if various tests are needed to determine the formability index. Conversely, the Fukui test [84], based on a conical die deep drawing, gives a measure of the material drawability with only one test, but its results are less accurate than those of the Swift test. Since many forming operations involve both stretching and drawing, combined tests were developed. The Swift round-bottomed cup test [45] resembles the Swift cup test except that the punch has a hemispherical head that causes the sheet stretching besides the draw-in of the flange into the cup wall. Furthermore, the Fukui conical cup test uses the same tools as the Fukui test apart from the hemispherical shape of the punch.

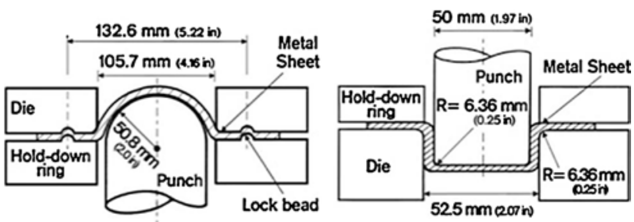

Fig. 25. Sketch of the limit dome height test on the left [21], and sketch of the Swift cup test on the right [212].

3.4.3. Tests to determine the Forming Limit Diagrams

Basically, two different types of tests are currently used to draw FLDs, namely stretching tests producing out-of-plane deformation, and tests producing only in-plane deformation. For both the test types, the sheet is marked with a grid pattern, and then deformed. The deformation of the grid pattern is measured in those regions where either necking or fracture occurs, giving the values of the major and minor strains. In the stretching tests, sheets of different widths are clamped between the die and the blank-holder and stretched by the action of a punch, providing adequate lubrication between the sheet and the punch. The Nakajima test [137] uses a hemispherical punch, a circular die, and simple rectangular sheets, providing a simple way to cover the whole FLD domain, but with some difficulties in measurement caused by the bending effect due to the punch curvature. Among the tests producing in-plane deformation, the Marciniak test [169] is the most used: it adopts punches of different cross sections (circular, elliptical, rectangular) with a central hole and sheets of different widths. The Marciniak test provides better accuracy in measurement, but has negative aspects, such as the complex shape of the tools, the need for a carried blank, and the limitation in the thickness of the sheets that can be tested. The comparison of results between the two types of tests shows a close agreement for negative minor strains, whereas the stretching methods give slightly higher values of formability for plane strain and positive minor strains.

Over the past few years, automated optical strain measurement methods, such as Digital Image Correlation (DIC), have been integrated into such testing methods, allowing for the direct and accurate measurement of the three dimensional strains on the metal sheet surface with minimal surface preparation [230]. The primary limitation of the mentioned forming limit measurement techniques is that the strain field, rather than the stress one, is the only directly measureable quantity that can be obtained, whereas stress measurements are often convoluted with issues related to friction and evolving geometry during testing. To overcome this limitation, in [83] a stress measurement technique using X-Ray Diffraction (XRD) was integrated within a Marciniak in-plane biaxial stretching testing setup to directly measure multi-axial stresses: an image of the testing setup is shown in Fig. 26. This advanced testing setup demonstrated to be an effective measurement method for the direct characterization of the evolving yield loci of sheet metals, such as the AA5754-O [120].

An additional advancement linked to conventional forming limit measurement techniques is related to the in situ measurement of microstructural features. By using a miniaturized Marciniak testing setup, in [216] the entire stretching test was conducted inside the chamber of a Scanning Electron Microscope (SEM) in order to probe micron-scale strain fields, damage mechanisms, and microstructure evolution. Fig. 27 shows the testing setup and some results in terms of strain field, damage evolution, and microstructural features.

In [179], the failure prediction in the region of biaxial stretching of the FLD was improved thanks to the implementation of a new

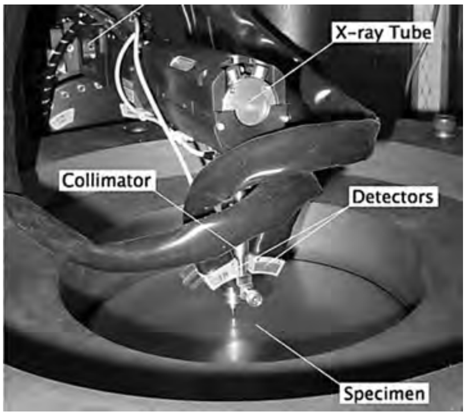

Fig. 26. Experimental setup for the in situ stress measurement in a Marciniak test [83].

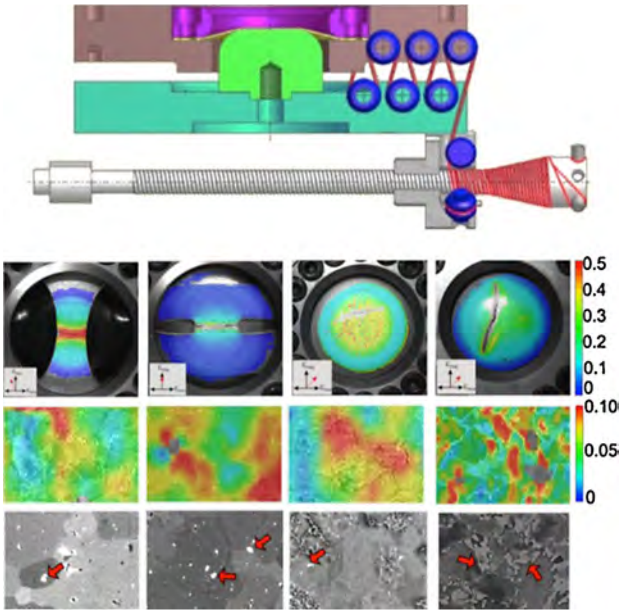

Fig. 27. Experimental setup for the in situ measurement of the strain field, damage evolution, and microstructural features during a Marciniak test carried out inside a SEM [216].

time-dependent analysis method that made use of a regression analysis of the strain rate to automatically detect the onset of necking. The proposed method also enhances the reproducibility of the tests by eliminating the impact of the user's decisions.

In [30] a new method for the experimental determination of the FLDs was proposed, based on the hydraulic bulging of two specimens. The most significant advantages of the method are its capability of investigating the whole strain range specific to the sheet metal forming processes, the simplicity of the equipment, and the reduction of the parasitic effects induced by the friction, as well as the occurrence of the necking in the polar region.

3.4.4. *Other formability tests*

A non-conventional testing equipment to study the different failure mechanisms arising due to the imposed stress state was proposed in [77]: a Continuous Bending under Tension (CBT) test was developed to generate cyclic stretch-bending.

An interesting aspect related to the formability characterization can be seen in the field of incremental sheet forming. Since the deformation mechanisms in incremental forming differ from the ones of conventional deep drawing [76,125], there is a need for alternative characterization and evaluation methods. In [81], different tests to achieve different strain paths and states were developed for that purpose, obtaining FLDs that are quite different from the conventionally obtained curves. Another strategy is proposed in [119] to test the thinning limits of sheet metals for negative incremental forming: to achieve this, an axi-symmetric geometry was designed with a side wall slope varying with depth, therefore leading to differential thinning along the side wall in the depth direction. In [104] similar geometries were used and several tests were performed to derive a response surface for predicting the process forming limits. Some research studies state that the formability enhancement in incremental sheet forming is still limited by the sheet necking but improved thanks to different stabilizing effects [125], whereas others debate the necking avoidance before fracture [76]. In [206], a unified theory is proposed, based on a critical threshold of a process geometrical parameter.

Tube expansion tests are also applied to study the formability of sheet metals. In [147], a new multi-axial tube expansion test was proposed: a multi-axial tube expansion testing machine was developed that can realize different principal stress or strain paths by controlling the axial force and internal pressure. The required tubular specimens are fabricated from the sheets by roll bending and laser welding. The proposed setup makes it possible to obtain the FLD and FLSD at the same time since the stresses can also be calculated analytically. However, though the method was deemed appropriate for large strain ranges, the in-plane cruciform test method was still suggested to characterize behaviour more accurately at low levels of strain [147]. Similar research subjects also appear in the field of hydroforming of tubular products. In [208] a new equipment and testing method for determining both the flow stress and formability of tubes was proposed, making use of a simple stand-alone hydraulic bulging fixture that enables testing under bi-axial stress state.

3.4.5. *Formability tests at elevated temperature*

Some of the formability tests presented above were modified and adapted in terms of equipment and testing procedures to enable the sheet metal formability limits at elevated temperature to be determined.

The bulge test was carried out at different strain rates on superplastic aluminium alloy sheets in [31], by using different punch geometries and varying the process parameters, namely temperature, strain rate, and counter-pressure: it was reported that the shape of the superplastic FLDs was different from the shape of the conventional FLDs.

In the field of hot stamping of high strength steel sheets, a new experimental procedure was proposed in [34], based on two complementary tests aimed at analysing the phase transformation kinetics and strain paths that lead to necking and then fracture. The proposed experimental setup has a control system to keep the temperature of the sheet constant during the test by using induction heating to heat the blank, cartridge heaters to heat the tools, and air nozzles to cool the blank to the desired testing temperature. A similar testing setup was also used to obtain the formability of magnesium alloys as a function of the temperature, strain and strain rate in [7]. In [49], the formability of magnesium alloys at high temperature was also studied with regard to the sheet rolling direction, leading to the conclusion that the formability in the rolling direction is higher than the one in the transverse direction.

Recent studies addressed the hot formability curves for the AZ31B magnesium alloys at near-constant strain rates, by utilizing the pneumatic stretching test. In [3] a methodology using pneumatic bulging for assessing formability and limiting strains of sheet metals at elevated temperatures is discussed: the study was shown to rectify the major limitations of mechanical stretching tests, mainly in terms of strain rate control, and proved to be capable of eliminating frictional effects at very high temperatures. In spite of that, the formability curves extracted via pneumatic stretching are confined to the right side of the forming limit diagram, since the test cannot generate negative minor strains. To overcome this limitation, in a more recent study [4], a hybrid numerical/experimental approach that targeted the development of near-constant strain rate loading paths in mechanical stretching tests was developed. The proposed approach takes into consideration the strain localization in the sheet, which is found to have a significant impact on the strain rate evolution, and hence on the testing speed. Several specimen geometries, corresponding to different major-to-minor strain ratios, were studied, and the results are used to construct complete FLDs as shown in Fig. 28.

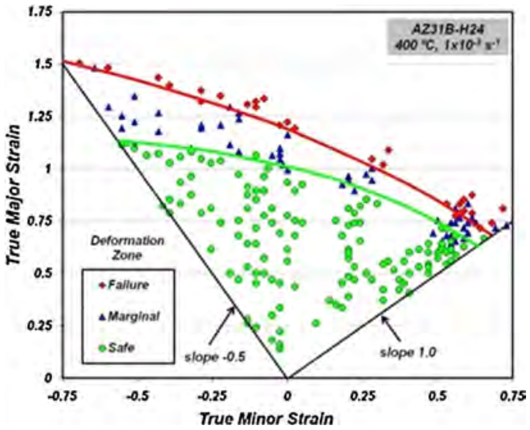

Fig. 28. FLD obtained at constant temperature and strain rate through mechanical stretching [4].

3.4.6. Formability tests at high strain rate

High values of strain rate can affect the sheet metal formability limits. In [138], static and high-speed FLDs obtained through punch-stretch tests with circular and square-shaped specimens are compared; the high-speed tests were performed on a crash testing machine with a high-speed forming jig. As a result of this comparison it was clear that the high-speed FLDs are lower than the static ones in the biaxial stretch forming region.

In [213], a deep drawn part was produced by using a testing equipment for impulse forming integrated with a deep drawing punch: after forming a circular cup with a soft punch edge radius, the impulse forming was applied to sharpen the edge radius of the cup. This method enabled strain values to be attained that were not possible using the single deep drawing process, and showed that, even if the static forming capacity of the material was fully used by deep drawing, the impulse forming can form the material further, and thereby significantly exceed the static forming limit curve (see Fig. 29). A photon doppler velocimeter is introduced in [65] to characterize the material behaviour under electro-magnetic forming conditions.

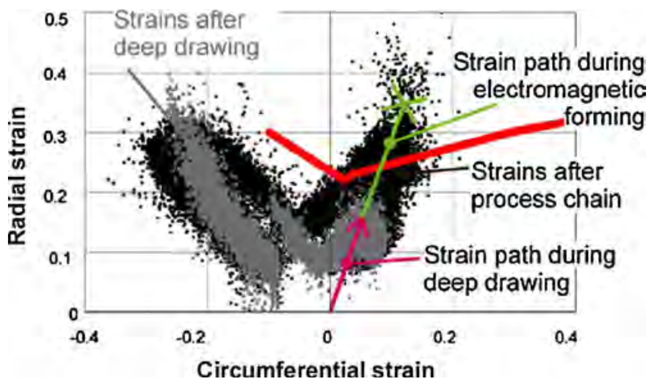

Fig. 29. Improvement of the sheet formability thanks to electromagnetic forming after deep drawing [213].

3.4.7. The benefits and limitations to formability testing

Several tests are commonly used to determine the forming limits of sheet metals, some of them widely diffused and recommended by international standards. They are characterized by a different degree of abstraction, ranging from material-testing type, such as the intrinsic tests, to physical simulation experiments, such as the simulative tests, which however, cannot assure the transferability of the results to stamping processes other than the one they replicate. Even if they are able to cover almost the whole range of strain states arising in sheet forming operations, the tests devoted to the determination of the FLDs show several shortcomings, above all the dependence of their results on different parameters, such as the blank thickness, anisotropy, imposed strain path.

On the other hand, the introduction of innovative forming processes has pushed either the development of new formability tests or the adaption of existing ones to replicate the new process conditions, forcing the implementation of new measuring techniques and data analyses, which, in turn, could be of benefit also to the more conventional tests.

4. Discussion and outlook

Since the nineteenth century, the response of a metal sheet subjected to sheet working conditions has been afforded much attention, especially as regards hardening, anisotropic and formability behaviour, giving raise to a large amount of literature. A wide range of tests is actually available to reproduce the material behaviour as well as numerous models to describe the different phenomena that characterize the metal response. For this reason, the last two chapters have given an overview of both the most consolidated and the emerging tests and models on the basis of the recent advent of new sheet materials and processes. The major evolution trend in modelling research appears to be the progressive shift from phenomenological to physical modelling, whereas testing is moving from uniaxial towards multi-axial loading conditions, able to reproduce industrial operating conditions more faithfully.

This last chapter is divided into three parts: the first one summarizes the evidence provided in the paper of how well existing models and tests meet the needs of the sheet forming industry; the second one deals with the need to fully integrate the materials design stage with process design in order to improve both the process and the product performances; the third part lists the challenges in testing and modelling the material response in sheet forming.

4.1. Do current models and tests meet the needs of the sheet metal forming industry?

Numerical simulation tools are more and more widespread in the sheet metal forming industry, which is requiring more and more sophisticated numerical models to simulate forming processes characterized by complex strain paths and severe process conditions, in order to provide more accurate predictions in terms of geometrical features and post-forming characteristics of the formed components. This requirement can be fully fulfilled only through the implementation of models of sheet metal behaviour and forming limits general enough to be able to reproduce the material response under any process conditions. Phenomenological and physical models answering to this demand have been already implemented to a certain extend, but their application is still limited in practice. This is mainly due to the fact that material data available for the model calibration are generally obtained through conventional uniaxial tests, which forces to use of single models that can be calibrated through these tests. There is then a strong need to provide industry with not only adequate models, but also with testing procedures and related material data that may be of help in calibrating the required models.

4.2. Future needs in material design for forming

Materials design is typically a goal-driven process by which the properties and response of a material can be modified for a given application. In [60], the need is contemplated for the development and implementation of novel materials capable of increasing the process capability window and of helping to provide an answer to the question: how do we produce more with less? The tremendous advances in materials and manufacturing technologies have occurred in parallel in the last decades, all too clearly evident due to the increased product performance and productivity. However, most of those advances have occurred in separate fields, e.g. materials science and mechanical engineering. Engineers optimize manufacturing processes relying on available materials. For example, the automotive industry went through a large 10–15 year learning curve when aluminium alloys were introduced for lightweight applications. The forming of composites is still in its development stage as most of the composites have been developed for other processes, such as resin transfer moulding or autoclave processes. There are very few instances, if any, in which material design, product design and manufacturing process design are performed concurrently to meet the requirements in an "optimal" sense. Yet it is clear that these three aspects are intricately interwoven. The reason for this situation rests in existing gaps in the understanding of the intricate relationships between material properties and responses to the different manufacturing processes used.

Here, we call for a step more advanced than what was expressed up to now, i.e., fully integrating material design and forming processes. This integrated approach is necessary as we have arrived at the conclusion that the process-level performance is a necessary consideration for the design process since: (1) Processing changes the microstructure of the material and hence changes its properties; (2) Final product performance is based on both the properties of the synthesized material and also the processing techniques used; and (3) Designing materials to have improved processability in a particular process will allow for faster deployment of multiple new products by increasing the process capability window.

Through in-depth understanding of the mechanics of existing processes we can redirect materials design to give improved process-level performance, leading to materials with enhanced processability, i.e., formability, machinability, etc. As an example, Fig. 30 illustrates a successful material design process [108] that was developed from a concept to flight qualification in only 8.5 years using only 5 prototype alloys, saving $50 million compared to the traditional empirical process.

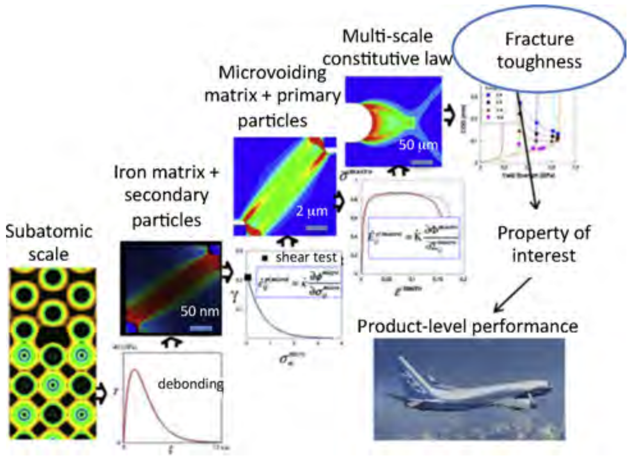

Fig. 30. Illustration of multi-scale material design [108].

Note that the complexity of the above example increases as more advanced forming technologies are involved, for example, hybrid forming processes, forming of heterogeneous or gradient materials, or electrically-assisted processes. To shorten the materials design cycle, it is essential to understand material deformation mechanics from nano-scale for precipitates, for example, to macroscopic characterization of large deformation. Topics discussed in this paper can serve as the bridging mechanism in the integrated material design for forming.

4.3. Challenges in current and future scientific and technological research

In recent years, on one hand, it is evident an increasing trend in developing new tests and models and/or extending the capabilities of the existing ones in order to reproduce more and more closely the phenomenology underlying both the traditional and new sheet processes and metals we are nowadays facing.

This is orienting the research efforts towards:

- developing more sophisticated testing equipment and procedures, integrating different measuring devices with the aim of acquiring as much as possible information within a single test;
- developing physically-based models capable of describing the physical phenomena occurring during the forming process, often coupled with evolutionary equations of the microstructural features;
- extending and improving the current knowledge about new classes of materials that are increasingly being processed under conditions that are typical of sheet forming (e.g. polymers, composites, sandwich structures), giving rise to new fields of investigation for bridging the gap between material behaviour and process performance;
- extending the current testing standards or developing new ones that are applicable to the emerging processes, especially those that are already industrially applied (e.g. sheet forming at elevated temperature, incremental sheet forming).

On the other hand, the request to simplify the testing approaches and the modelling techniques is even more demanding, coming not only from the industry, which often still relies only on trial-and-error approaches, but also represents an evolutionary trend in the scientific community that attempts to provide unified theories capable of linking the basic knowledge of materials science and the different phenomena arising during the forming processes. This scenario brings out new challenges, forcing us to:

- rethink testing and modelling approaches that are considered already consolidated, by taking hints from other research fields, such as fracture mechanics and crystal plasticity;
- develop models reproducing the phenomenon, either at a macro- or a micro-scale, which should be general enough to be applicable to different states of stress and strain. These models should be not only accurate in predicting the material behaviour, but also prove to have transferability characteristics;
- couple the material-, process-, and product-oriented modelling domains in order to offer models capable of predicting material behaviour and product characteristics during and after the sheet forming stages;
- provide useful guidelines to process designers for calibrating the numerical models, using the most suitable models on the basis of the material/process pair and the adopted design strategies, as well as good practice guides to the industrial practitioners for a fast in-line verification of product quality.

Acknowledgments

The authors wish to thank the following persons for their contributions in the preparation of the paper.

From CIRP: J. Allwood, University of Cambridge, UK; P. Groche, University of Darmstadt, Germany; L. Fratini and F. Micari, University of Palermo, Italy; L. Madej, Akademia Gorniczo-Hutnicza, Poland; P. Martins, Univ. of Lisboa, Portugal; K. Mori, Toyohashi University, Japan; R. Shivpuri, The Ohio State University, USA.

From other institutions: J. Puerta-Velasquez, Arcelor-Mittal, France; A. Sterzing, University of Chemnitz, Germany; S. Suttner, Friedrich-Alexander-Universität Erlangen-Nürnberg, Germany W. Volk, University of Munich, Germany.

References

[1] Abu-Farha FK (2007) *Integrated Approach to the Superplastic Forming of Magnesium Alloys*, (PhD dissertation) University of Kentucky.
[2] Abu-Farha F, Hector Jr LG, Khraisheh M (2009) Cruciform-Shaped Specimens for Elevated Temperature Biaxial Testing of Lightweight Materials. *JOM – Aluminium: Shaping and Forming* 61(8):48–56.
[3] Abu-Farha F, Shuaib N, Khraisheh M, Weinmann K (2008) Limiting Strains of Sheet Metals Obtained by Pneumatic Stretching at Elevated Temperatures. *CIRP Annals – Manufacturing Technology* 57(1):275–278.
[4] Albakri M, Abu-Farha F, Khraisheh M (2013) A New Combined Experimental Numerical Approach to Evaluate Formability of Rate Dependent Materials. *International Journal of Mechanical Sciences* 66:55–66.
[5] Al-Nasser A, Yadav A, Pathak P, Altan T (2010) Determination of Flow Stress of Five AHSS Sheet Materials (DP600 DP780 DP780-CR DP780-HY and TRIP780) Using Uniaxial Tensile and Biaxial Viscous Pressure Bulge (VPB) Tests. *Journal Materials Processing Technology* 210(3):429–436.
[6] Alves LM, Nielsen CV, Martins PAF (2011) Revisiting the Fundamentals and Capabilities of the Stack Compression Test. *Experimental Mechanics* 51:1565–1572.
[7] Ambrogio G, Bruni C, Bruschi S, Filice L, Ghiotti A, Simoncini M (2008) Characterisation of AZ31B Magnesium Alloy Formability in Warm Forming Conditions. *International Journal of Material Forming* 1:205–208.
[8] An Y, Vegter H, Heijne J (2009) Development of Simple Shear Test for the Measurement of Work Hardening. *Journal of Materials Processing Technology* 209:4248–4254.
[9] Armstrong PJ, Frederick CO (1966) A Mathematical Representation of the Multiaxial Bauschinger Effect. *CEGB Report RD/B/N73 1 Central Electricity Generating Board*, .
[10] Arrieux R, Bedrin C, Boivin M (1982) Determination of an Intrinsic Forming Limit Stress Diagram for Isotropic Sheets. *Proc of 12th IDDRG Congress*, 61–71.
[11] Asaro RJ (1985) Material Modelling and Failure Modes in Metal Plasticity. *Mechanics of Materials* 4:343–373.
[12] ASTM E2218-02 (2008) *Standard Test Method for Determining Forming Limit Curves*.
[13] ASTM Standard B 831-05 (2005) *Standard Test Method for Shear Testing of Thin Aluminium Alloy Products*, ASTM Standards, West Conshohocken, PA, USA.
[14] ASTM E290 (2013) *Standard Test Methods for Bend Testing of Material for Ductility*.
[15] ASTM E643 (2009) *Standard Test Method for Ball Punch Deformation of Metallic Sheet Material*.
[16] ASTM E8 (2013) *Standard Test Methods for Tension Testing of Metallic Materials*.
[17] Atkins AG (1996) Fracture in Forming. *Journal of Materials Processing Technology* 56:609–618.
[18] Atkins AG, May YW (1987) Fracture Strains in Sheet Metal Forming and Specific Essential Work at Fracture. *Engineering Fracture Mechanics* 27(3):291–297.
[19] Avrami M (1939) Kinetics of Phase Change. I: General Theory. *Journal of Chemical Physics* 7:1103.
[20] Avrami M (1940) Kinetics of Phase Change. II: Transformation–Time Relations for Random Distribution of Nuclei. *Journal of Chemical Physics* 8:212.
[21] Ayres RA, Brazier WG, Sajewski VF (1979) Evaluating the Limiting Dome Height Test as a New Measure of Press Formability. *Journal of Applied Metalworking* 1(1):41–49.
[22] Bae DH, Ghosh AK (2003) A Planar Simple Shear Test and Flow Behaviour in a Superelastic Al–M Alloy. *Metallurgical and Materials Transactions A* 34:2465–2471.
[23] Banabic D (2010) A Review on Recent Developments of Marciniak–Kuczynski Model. *Computer Methods in Materials Science* 10(4):1–13.
[24] Banabic D, Aretz H, Comsa DS, Paraianu L (2005) An Improved Analytical Description of Orthotropy in Metallic Sheets. *International Journal of Plasticity* 21:493–512.
[25] Banabic D, Balan T, Comsa DS (2000) A New Yield Criterion for Orthotropic Sheet Metals Under Plane–Stress Conditions. *The 7th Conf "TPR2000"Cluj Napoca*, 217–224.
[26] Banabic D, Bunge HJ, Pöhlandt K, Tekkaya AE (2000) in Banabic D, (Ed.) *Formability of Metallic Materials*, Springer, Berlin/Heidelberg.
[27] Banabic D, Comsa DS, Sester M, Selig M, Kubli W, Mattiasson K, Sigvant M (2008) Influence of Constitutive Equations on the Accuracy of Prediction in Sheet Metal Forming Simulation. in Hora P, (Ed.) *Proc 7th Int Conf NUMISHEET 2008*, 37–42.
[28] Banabic D, Kuwabara T, Balan T, Comsa DS (2004) An Anisotropic Yield Criterion for Sheet Metals. *Journal of Materials Processing Technology* 157(158):462–465.
[29] Banabic D, Kuwabara T, Balan T, Comsa DS, Julean D (2003) Non-Quadratic Yield Criterion for Orthotropic Sheet Metals Under Plane-Stress Conditions. *International Journal of Mechanical Sciences* 45:797–811.
[30] Banabic D, Lazarescu L, Paraianu L, Ciobanu I, Nicodim I, Comsa DS (2013) Development of a New Procedure for the Experimental Determination of the Forming Limit Curves. *CIRP Annals – Manufacturing Technology* 62(1):255–258.
[31] Banabic D, Vulcan M, Siegert K (2005) Bulge Testing Under Constant and Variable Strain Rates of Superplastic Aluminium Alloys. *CIRP Annals – Manufacturing Technology* 54(1):205–208.
[32] Bao Y (2003) *Prediction of Ductile Crack Formation in Uncracked Bodies*, (PhD thesis) Massachusets Institute of Technology.
[33] Bao Y, Wierzbicki T (2004) On Fracture Locus in the Equivalent Strain and Stress Triaxiality Space. *International Journal of Mechanical Sciences* 46(1):81–98.
[34] Bariani PF, Bruschi S, Ghiotti A, Turetta A (2008) Testing Formability in the Hot Stamping of HSS. *CIRP Annals – Manufacturing Technology* 57(1):265–268.
[35] Bariani PF, Dal Negro T, Bruschi S (2004) Testing and Modelling of Materials Response to Deformation. *CIRP Annals – Manufacturing Technology* 53(2):1–22.
[36] Barlat F, Aretz H, Yoon JW, Karabin ME, Brem JC, Dick RE (2005) Linear Transformation-Based Anisotropic Yield Functions. *International Journal of Plasticity* 21:1009–1039.
[37] Barlat F, Brem JC, Yoon JW, Chung K, Dick RE, Lege DJ, Pourboghrat F, Choi S-H, Chu E (2003) Plane Stress Yield Function for Aluminium Alloy Sheets Part I: Formulation. *International Journal of Plasticity* 19:1297–1319.
[38] Barlat F, Lian J (1989) Plastic Behaviour and Stretchability of Sheet Metals (Part 1) A Yield Function for Orthotropic Sheet Under Plane Stress Conditions. *International Journal of Plasticity* 5:51–56.
[39] Bauer M (1987) Faltenbildung beim ebenen Torsionsversuch. *Archive of Applied Mechanics* 57:39–50.
[40] Bauschinger J (1886) *Über die Veränderung der Elastizitätsgrenze und der Festigkeit des Eisens und Stahls durch Strecken und Quetschen durch Erwärmen und Abkühlen und durch oft mal wiederholte Beanspruchung Mitteilung XV aus dem Mechanisch Technischen Laboratorium der Königlichen TH in München 13*1–116.
[41] Boehler JP, Demmerle S, Koss S (1994) A New Direct Biaxial Testing Machine for Anisotropic Materials. *Experimental Mechanics* 34(1):1.
[42] Boers SHA, Geers MGD, Kouznetsova VG (2010) Contactless and Frictionless Pure Bending. *Experimental Mechanics* 50:683–693.
[43] Boger R, Wagoner R, Barlat F, Lee M, Chung K (2005) Continuous, Large Strain, Tension/Compression Testing of Sheet Material. *International Journal of Plasticity* 21:2319–2343.
[44] Bouvier Alves JL, Oliveira MC, Menezes LF (2005) Modelling of Anisotropic Work-Hardening Behaviour of Metallic Materials Subjected to Strain-Path Changes. *Computational Materials Science* 32:301–315.
[45] Boyles MW, Chilcott HS (1982) Recent Developments in the Use of the Stretch-Draw Test. *Sheet Metal Industry* 59:149–156.
[46] Brieu M, Diani J, Bhatnagar N (2006) A New Biaxial Tension Test Fixture for Uniaxial Testing Machine – A Validation for Hyperelastic Behaviour of Rubberlike Materials. *Journal of Testing and Evaluation* 35(4):1–9.
[47] Brosius A, Yin Q, Güner A, Tekkaya AE (2011) A New Shear Test for Sheet Metal Characterization. *Steel Research International* 82(4):323–328.
[48] Brozzo P, Deluca B, Rendina R (1972) A New Method for the Prediction of Formability Limits in Metal Sheets. *Proc. of the Seventh Biannual Conference of IDDRG*.
[49] Bruni C, Forcellese A, Gabrielli F, Simoncini M (2010) Effect of Temperature, Strain Rate and Fibre Orientation on the Plastic Flow Behaviour and Formability of AZ31 Magnesium Alloy. *Journal of Materials Processing Technology* 210:1354–1363.
[50] Brünig M (2003) An Anisotropic Ductile Damage Model Based on Irreversible Thermodynamics. *International Journal of Plasticity* 19:1679–1713.
[51] Brünig M, Ricci S (2005) Nonlocal Continuum Theory of Anisotropically Damaged Metals. *International Journal of Plasticity* 21:1346–1382.
[52] Caceres CH, Wilkinson DS (1984) Large Strain Behaviour of a Superplastic Copper Alloy – I. Deformation. *Acta Metallurgica* 32:415–422.
[53] Canpolat A (2013) *Experimentelle und numerische Bewertung der Fließortbestimmung mittels Kreuzzugversuch*, (PhD thesis) Technische Universität Dortmund.
[54] Cao J, Lee W, Cheng HS, Seniw M, Wang H-P, Chung K (2009) Experimental and Numerical Investigation of Combined Isotropic-Kinematic Hardening Behavior of Sheet Metals. *International Journal of Plasticity* 25:942–972.
[55] Cazacu O, Barlat F (2001) Generalization of Drucker's Yield Criterion to Orthotropy. *Mathematics and Mechanics of Solids* 6:613–630.
[56] Cazacu O, Barlat F (2003) Application of the Theory of Representation to Describe Yielding of Anisotropic Aluminium Alloys. *International Journal of Engineering Science* 41:1367–1385.
[57] Cazacu O, Plunkett B, Barlat F (2006) Orthotropic Yield Criterion for Hexagonal Close Packed Metals. *International Journal of Plasticity* 22:1171–1194.
[58] Chaboche JL (1986) Time Independent Constitutive Theories for Cyclic Plasticity. *International Journal of Plasticity* 2:149.
[59] Chaboche JL (1989) A New Constitutive Framework to Describe Limited Ratchetting Effects. in Khan AS, Tokuda M, (Eds.) *Plasticity'89, Tsu, Japan*, 211–214.
[60] Chryssolouris G, Papakostas N, Mavrikios D (2008) A Perspective on Manufacturing Strategy: Produce More with Less. *CIRP Journal of Manufacturing Science and Technology* 1:45–52.
[61] Chu Y, Lee R, Psyk V, Tekkaya AE (2012) Determination of the Flow Curve at High Strain Rates Using Electromagnetic Punch Stretching. *Journal of Materials Processing Technology* 212:1314–1323.
[62] Chung K, Lee M-G, Kim D, Kim C, Wenner ML, Barlat F (2005) Spring-back Evaluation of Automotive Sheets Based on Isotropic-Kinematic Hardening Laws and Non-Quadratic Anisotropic Yield Functions, Part I: Theory and Formulation. *International Journal of Plasticity* 21:861.
[63] Cockcroft MG, Latham DJ (1968) Ductility and the Workability of Metals. *Journal of the Institute of Metals* 96:33–39.
[64] Comsa DS, Banabic D (2008) Plane-Stress Yield Criterion for Highly-anisotropic Sheet Metals. in Hora P, (Ed.) *Proc 7th Int Conf NUMISHEET 2008*, 43–48.
[65] Daehn G, Zhang YGS, Banik K, Vivek A, Johnson J, Taber G, Fenton GHI, L'Eplattenier P (2008) Coupling Experiment and Simulation in Electro-magnetic Forming Using Photon Doppler Velocimetry. *Proceedings of the 3rd International Conference on High Speed Forming – ICHSF*, 35–44.
[66] Dafalias YF, Popov EP (1976) Plastic Internal Variables Formalism of Cyclic Plasticity. *ASME Journal of Applied Mechanics* 43:645.
[67] Devenpack ML, Richmond O (1983) Limiting Strain Tests for In-Plane Sheet Stretching Novel Techniques in Metal Deformation Testing. *Metallurgical Society* 79–88.

[68] DIN 50106:1978-12 (2009) *Prüfung metallischer Werkstoffe; Druckversuch; German version*, Deutsches Institut für Normung eV/Beuth, Berlin.
[69] Doege E, Meyer-Nolkemper H, Saeed I (1996) *Fließkurvenatlas metallischer Werkstoffe*, Hanser-Verlag, München.
[70] Doege E, Sebastian W, Droder K, Kurz G (2001) Increased Formability of Mg-Sheets using Temperature Controlled Deep Drawing Tools. *Innovations in Processing and Manufacturing of Sheet Materials, TMS Annual Meeting*, 53–60.
[71] Doig M, Kaupper M, Kraska M, Eißer G, Merklein M, Roll K, Keßler L (2010) Inverse Identification of Kinematic Hardening Parameters with Bending Tests. in Kolleck R, (Ed.) *Proceedings of the 50th Conference of IDDRG*, 555–564.
[72] Drucker DC (1949) Relation of Experiments to Mathematical Theories of Plasticity. *Journal of Applied Mechanics* 16:349–357.
[73] Duncan JL, Kolodziejski J, Glover G (1976) Bulge Testing as an Aid to Formability Assessment. *Proc of the 9th Biennial Congress of International Deep Drawing Research Group*, 131–150.
[74] Easterling RG (2001) Quantifying the Uncertainty of Computational Predictions. *Proc. of the 2001 SEM Annual Conference*.
[75] Embury JD, Duncan JL (1981) Formability Maps. *Annual Review of Materials Science* 11:505–521.
[76] Emmens W, van den Boogaard AH (2009) An Overview of Stabilizing Deformation Mechanisms in Incremental Sheet Forming. *Journal of Materials Processing Technology* 209:3688–3695.
[77] Emmens W, van den Boogaard AH (2011) Cyclic Stretch-Bending: Mechanics, Stability and Formability. *Journal of Materials Processing Technology* 211:1965–1981.
[78] Fansi J, Balan T, Lemoine X, Maire E, Landron C, Bouaziz O, Bettaieb MB, Habraken AM (2013) Numerical Investigation and Experimental Validation of Physically Based Advanced GTN Model for DP Steels. *Materials Science and Engineering A* 569:1–12.
[79] Ferron G, Makinde A (1988) Design and Development of a Biaxial Strength Testing Device. *Journal of Testing and Evaluation* 16(3):253–256.
[80] Field JE, Walley SM, Proud WG, Goldrein HT, Siviour CR (2004) Review of Experimental Techniques for High Rate Deformation and Shock Studies. *International Journal of Impact Engineering* 30:725–775.
[81] Filice L, Fratini L, Micari F (2002) Analysis of Material Formability in Incremental Forming. *CIRP Annals – Manufacturing Technology* 51(1):199–202.
[82] Fischer FD, Reisner G, Werner E, Tanaka K, Cailletaud G, Antretter T (2000) A New View on Transformation Induced Plasticity (TRIP). *International Journal of Plasticity* 16(7–8):723–748.
[83] Foecke T, Iadicola MA, Lin A, Banovic SW (2007) A Method for Direct Measurement of Multiaxial Stress–Strain Curves in Sheet Metal. *Metallurgical and Materials Transactions A* 38:306–313.
[84] Fukui S (1939) Researches on the Deep-Drawing Process. *Institute of Physical and Chemical Research* 34:1422–1527.
[85] Geiger M, van der Heyd G, Merklein M, Hußnätter W (2005) Novel Concept of Experimental Setup for Characterisation of Plastic Yielding of Sheet Metal at Elevated Temperatures. *Journal of Advanced Materials Research* 6(8):657–664.
[86] Geng L, Shen Y, Wagoner R (2002) Anisotropic Hardening Equations Derived from Reverse-Bend Testing. *International Journal of Plasticity* 18:743–767.
[87] Gese H, Dell H, Keller S, Yeliseyev V. (2003) Ermittlung von Fließwiderstandskurven bei großen Formänderungen für die Blechumformsimulation. Frenz H Wehrstadt A (Hrsg): Kennwertermittlung für die Praxis Weinheim: Wiley-VCH 242–249.
[88] Ghiotti A, Bruschi S, Bariani PF (2007) Determination of Yield Locus of Sheet Metal at Elevated Temperatures: A Novel Concept for Experimental Set-Up. *Key Engineering Materials* 344:97–104.
[89] Gologanu M, Leblond JB, Devaux J (1993) Approximate Models for Ductile Metals Containing Non-Spherical Voids – Case of Axisymmetric Prolate Ellipsoidal Cavities. *Journal of the Mechanics and Physics of Solids* 41(11):1723–1754.
[90] Gologranc F (1975) *Evaluation of the Flow Stress Curve with the Continuous Hydraulic Bulge Test*, (PhD dissertation) Institute for Metal Forming Technology, University of Stuttgart, Germany.
[91] Goodwin GM (1968) Application of Strain Analysis to Sheet Metal Forming Problems. *Press Shop Society of Automotive Engineers Tech Paper no 680093*, .
[92] Gotoh M (1985) A Class of Plastic Constitutive Equations with Vertex Effect—IV: Applications to Prediction of Forming Limit Strains of Metal Sheets Under Non-Proportional Loadings. *International Journal of Solids and Structures* 21:1149–1163.
[93] Graf A, Hosford WF (1993) Effect of Changing Strain Paths on Forming Limit Diagram of Al 2008-T4. *Metallurgical Transactions A* 24:2503–2512.
[94] Greenwood GW, Johnson RH (1965) The Deformation of Metals Under Small Stresses during Phase Transformation. *Proceeding of the Royal Society of London* 283(1394):403–422.
[95] Groche P, Huber R, Dörr J, Schmoeckel D (2002) Hydromechanical Deep-Drawing of Aluminium-Alloys at Elevated Temperatures. *CIRP Annals – Manufacturing Technology* 51(1):215–218.
[96] Güner A, Brosius A, Tekkaya AE (2009) Analysis of the Hydraulic Bulge Test with FEA Concerning the Accuracy of the Determined Flow Curves. *Key Engineering Materials* 410(411):439–447.
[97] Güner A, Brosius A, Tekkaya AE (2009) Experimental and Numerical Investigation of the Hydraulic Bulge Test for Accurate Flow Curve Determination. *Proceedings Int Deep Drawing Research Group IDDRG*.
[98] Güner A, Yin Q, Soyarslan C, Brosius A, Tekkaya AE (2011) Inverse Method for Identification of Initial Yield Locus of Sheet Metals Utilizing Inhomogeneous Deformation Fields. *International Journal of Material Forming* 4(2):121–128.
[99] Gurson AL (1977) Continuum Theory of Ductile Rupture by Void Nucleation and Growth – Part I. Yield Criteria and Rules for Porous Ductile Media. *Journal of Engineering Materials and Technology* 99:2–15.
[100] Gutscher G, Wu HC, Ngaile G, Altan T (2004) Determination of Flow Stress for Sheet Metal Forming Using the Viscous Pressure Bulge (VPB) Test. *Journal of Materials Processing Technology* 146:1–7.
[101] Ha J, Lee N-G, Barlat F (2013) Strain Hardening Response and Modelling of EDDQ and DP780 Steel Sheet Under Non-Linear strain Path. *Mechanics of Materials* 64:11–26.
[102] Haberfield AB, Boyles MW (1973) Laboratory Determined Forming Limit Diagrams. *Sheet Metal Industry* 50:400–411.
[103] Haddadi H, Bouvier S, Banu M, Maier C, Teodosiu C (2006) Towards an Accurate Description of the Anisotropic Behaviour of Sheet Metals Under Large Deformations: Modelling, Numerical Analysis and Identification. *International Journal of Plasticity* 22:2226–2271.
[104] Ham M, Jeswiet J (2007) Forming Limit Curves in Single Point Incremental Forming. *CIRP Annals – Manufacturing Technology* 56(1):277–280.
[105] Hannon A, Tiernan P (2008) A Review of Planar Biaxial Tensile Test Systems for Sheet Metal. *Journal of Materials Processing Technology* 198:1–13.
[106] Hansel AHC, Hora P, Reissner J (1998) Model for the Kinetics of Strain-Induced Martensitic Phase Transformation at Non-Isothermal Conditions for the Simulation of Sheet Metal Forming Processes with Metastable Austenitic Steels. in HuetinkBaajiens*Simulation of Material Processing: Theory, Methods and Applications*, Balkena, Rotterdam.
[107] Hanson KM, Hemez FM (2001) A Framework for Assessing Confidence in Computational Predictions. *Experimental Techniques* 25:50–55.
[108] Hao S, Moran B, Liu WK, Olson GB (2003) A Hierarchical Multi-Physics Model for Design of High toughness steels. *Journal of Computer Aided Materials Design* 10:99–142.
[109] Hecht J, Pinto S, Geiger M (2005) Determination of Mechanical Properties for the Hydroforming of Magnesium Sheets at Elevated Temperature. *Advanced Materials Research* 6(8):779–786.
[110] Hecker SS (1974) A Cup Test for Assessing Stretchability. *Metals Engineering Quarterly* 30–36.
[111] Hill R (1948) A Theory of the Yielding and Plastic Flow of Anisotropic Metals. *Proceedings of the Royal Society of London Series A: Mathematical and Physical Sciences* 193(1033):281–297.
[112] Hill R (1952) On Discontinuous Plastic States with Particular Reference to Localized Necking in Thin Sheets. *Journal of the Mechanics and Physics of Solids* 1:19–30.
[113] Hill R (1990) Constitutive Modelling of Orthotropic Plasticity in Sheet Metals. *Journal of the Mechanics and Physics of Solids* 38:405–417.
[114] Hockett JE, Sherby OD (1975) Large Strain Deformation of Polycrystalline Metals at Low Homologous Temperature. *Journal of the Mechanics and Physics of Solids* 23:87–98.
[115] Hollomon J (1945) Tensile deformation. *Transactions of the Society of Mining Engineers of American Institute of Mining* 162:268–272.
[116] Hosford WF (1979) On Yield Loci of Anisotropic Cubic Materials. *Proc 7th North American Metalworking Conf*, Dearborn, 191–197.
[117] Huber MT (1904) Przyczynek do Podstaw Wytorymalosci. *Czasopismo Techniczne* 22:34–81.
[118] Hußnätter W, Merklein M (2008) Characterization of Material Behavior Under Pure Shear Condition. *International Journal of Material Forming* 1(1):233–236.
[119] Hussain G, Gao L (2007) A Novel Method to Test the Thinning Limits of Sheet Metals in Negative Incremental Forming. *International Journal of Machine Tools and Manufacture* 47:419–435.
[120] Iadicola MA, Foecke T, Banovic SW (2008) Experimental Observations of Evolving Yield Loci in Biaxially Trained AA5754-O. *International Journal of Plasticity* 24:2084–2101.
[121] ISO 12004:2 (2008) *Metallic Materials – Sheet and Strip – Determination of Forming-limit Curves – Part 2: Determination of Forming-limit Curves in the Laboratory*.
[122] ISO/DIS 16808 (2013) *Metallic Materials – Sheet and Strip – Determination of Biaxial Stress–Strain Curve by Means of Bulge Test with Optical Measuring System. Under development*.
[123] ISO/DIS 16842 (2013) *Metallic Materials – Sheet and Strip – Biaxial Tensile Testing Method Using Cruciform Specimen. Under development*.
[124] Iwamoto T, Tsuta T (2000) Computational Simulation of the Dependence of the Austenitic Grain Size on the Deformation Behaviour of TRIP Steels. *International Journal of Plasticity* 16(7–8):791–804.
[125] Jackson K, Allwood J (2009) The Mechanics of Incremental Sheet Forming. *Journal of Materials Processing Technology* 209:1158–1174.
[126] Jarrar F, Abu-Farha F, Hector Jr L, Khraisheh M (2009) Simulation of High-Temperature AA5083 Bulge Forming with a Hardening/Softening Material Model. *Journal of Materials Engineering and Performance* 18:863–870.
[127] Johnson GR, Cook WH (1983) A Constitutive Model and Data for Metals Subjected to Large Strains, High Strain-Rates and High Temperature. *The 7th Symposium on Ballistic*, 541–547.
[128] Johnson GR, Cook WH (1985) Fracture Characteristics of Three Metals Subjected to Various Strains, Strain Rates, Temperatures and Pressures. *Engineering Fracture Mechanics* 21(1):31–48.
[129] Johnson W, Duncan JL (1963) A Rapid Method of Determining Stress–Strain Curves for Sheet Metalworking Using the Bulge Test. *Proc. of the 4th International MTDR Conference*Pergamon Press, Manchester.
[130] Kachanov LM (1961) On the Kinetics of Crack Growth. *PMM* 25(3):98–502.
[131] Kang J, Wilkinson DS, Wu PD, Bruhis M, Jain M, Embury JD, Mishra RK (2008) Constitutive Behavior of AA5754 Sheet Materials at Large Strains. *Journal of Engineering Materials and Technology* 130(3):41–45.
[132] Karbasian H, Tekkaya AE (2010) A Review on Hot Stamping. *Journal of Materials Processing Technology* 210:2103–2118.
[133] Kaya S, Altan T, Groche P, Klöpsch C (2008) Determination of the Flow Stress of Magnesium AZ31-O Sheet at Elevated Temperatures Using the Hydraulic

Bulge Test. *International Journal of Machine Tools and Manufacture* 48:550–557.
[134] Keeler SP, Backofen WA (1963) Plastic Instability and Fracture in Sheets Stretched Over Rigid Punches. *ASM Transactions* 56(1):25–48.
[135] Khan AS, Jackson KM (1999) On the Evolution of Isotropic and Kinematic Hardening with Finite Plastic Deformation, Part I: Compression/Tension Loading of OFHC Copper Cylinders. *International Journal of Plasticity* 15:1265.
[136] Khraisheh MK, Zbib HM, Hamilton CH, Bayoumi AE (1997) Constitutive Modeling of Superplastic Deformation. Part I: Theory and Experiments. *International Journal of Plasticity* 13:143–164.
[137] Kikuma T, Nakazima K (1971) Effects of the Deformation Conditions and Mechanical Properties on the Stretch Forming of Steel Sheets. *Transactions of the Iron and Steel Institute of Japan* 11:827–839.
[138] Kim S, Huh H, Bok H, Moon M (2011) Forming Limit Diagram of Auto-Body Steel Sheets for High-Speed Sheet Metal Forming. *Journal of Materials Processing Technology* 211:851–862.
[139] Kleiner M, Brosius A (2006) Determination of Flow Curves at High Strain Rates Using the Electromagnetic Forming Process and an Iterative Finite Element Simulation Scheme. *CIRP Annals – Manufacturing Technology* 55(1):267–270.
[140] Koistinen DP, Marburger RE (1959) A General Equation for Austenite–Martensite Transformation in Pure Carbon Steels. *Acta Metallurgica* 7:59–60.
[141] Koo JY, Young MJ, Thomas G (1980) On the Law of Mixtures in Dual-Phase Steels. *Metallurgical Transactions A* 11(5):852–854.
[142] Krieg RD (1975) A Practical Two Surface Plasticity Theory. *ASME Journal of Applied Mechanics* 42:641–646.
[143] Kuroda M, Tvergaard V (2000) Effect of Strain Path Change on Limits to Ductility of Anisotropic Metal Sheets. *International Journal of Mechanical Science* 42:867–887.
[144] Kurukuri S, van den Boogaard AH, Miroux A, Holmedal B (2009) Warm Forming Simulation of Al–Mg Sheet. *Journal of Materials Processing Technology* 209:5636–5645.
[145] Kuwabara T, Ikeda S, Kuroda K (1988) Measurement and Analysis of Differential Work Hardening in Cold-Rolled Steel Sheet Under Biaxial Tension. *Journal of Materials Processing Technology* 80(81):517–523.
[146] Kuwabara T, Kumano Y, Ziegelheim J, Kurosaki I (2009) Tension–Compression Asymmetry of Phosphor Bronze for Electronic Parts and its Effect on Bending Behavior. *International Journal of Plasticity* 25:1759–1776.
[147] Kuwabara T, Sugawara F (2013) Multiaxial Tube Expansion Test Method for Measurement of Sheet Metal Deformation Behavior Under Biaxial Tension for a Large Strain Range. *International Journal of Plasticity* 45:103–118.
[148] Kuwabara T, Van Bael A, Iizuka E (2002) Measurement and Analysis of Yield Locus and Work Hardening Characteristics of Steel Sheets with Different *r* Values. *Acta Materialia* 50:3717–3729.
[149] Lämmer H, Tsakmakis C (2000) Discussion of Coupled Elastoplasticity and Damage Constitutive Equations for Small and Finite Deformations. *International Journal of Plasticity* 16:496–523.
[150] Lange K (2002) *Umformtechnik: Handbuch für Industrie und Wissenschaft. Grundlagen*, 2nd ed. Springer, Berlin.
[151] Leblond JB, Devaux J, Devaux JC (1989) Mathematical Modelling of Transformation Induced Plasticity in Steels I. Case of Ideal-Plastic Phases. *International Journal of Plasticity* 5:551–573.
[152] Leblond JB, Mottet G, Devaux JC (1986) A Theoretical and Numerical Approach to the Plastic Behaviour of Steels During Phase-Transformation – II. Study of Classical Plasticity for Ideal-Plastic Phases. *Journal of the Mechanics and Physics of Solids* 34(4):411–432.
[153] Lecompte D, Smits A, Sol H, Vantomme J, Van Hemelrijck D (2007) Mixed Numerical-Experimental Technique for Orthotropic Parameter Identification Using Biaxial Tensile Tests on Cruciform Specimens. *International Journal of Solids and Structures* 44:1643–1656.
[154] Lee M-G, Wagoner RH, Lee JK, Chung K, Kim HY (2008) Constitutive Modelling for Anisotropic/Asymmetric Hardening Behavior of Magnesium Alloy Sheets. *International Journal of Plasticity* 24:545–582.
[155] Lemaitre J (1971) Evaluation of Dissipation and Damage in Metals. *Proceedings of ICM 1*, Kyoto, Japan.
[156] Lemaitre J (1996) *A Course on Damage Mechanics*, Springer-Verlag, Berlin.
[157] Lemaitre J, Desmorat R (2005) *Engineering Damage Mechanics*, Springer-Verlag, Berlin/Heidelberg.
[158] Lemonds J, Needleman A (1986) Finite Element Analysis of Shear Localization in Rate and Temperature Dependent Solids. *Mechanics of Materials* 5:339–361.
[159] Li J, Carsley JE, Stoughton TB, Hector LG, Hu SJ (2013) Forming Limit Analysis for Two-Stage Forming of 5182-O Aluminium Sheet with Intermediate Annealing. *International Journal of Plasticity* 45:21–43.
[160] Li S, Hoferlin E, Van Bael A, Van Houtte P, Teodosiu C (2003) Finite Element Modelling of Plastic Anisotropy Induced by Texture and Strain Path Change. *International Journal of Plasticity* 19:647–674.
[161] Li Y, Luo M, Gerlach J, Wierzbicki T (2010) Prediction of Shear-Induced Fracture in Sheet Metal Forming. *Journal of Materials Processing Technology* 210:1858–1869.
[162] LN 29512 (1969) *Kleine Zugproben. Deutsches Institut für Normung eV*, Beuth, Berlin.
[163] Ludwik P (2009) *Elemente der technologischen Mechanik*, Springer, Berlin.
[164] Magargee J, Cao J, Zhou R, McHugh M, Brink D, Morestin F (2011) Characterization of Tensile and Compressive Behavior of Microscale Sheet Metals Using a Transparent Microwedge Device. *Journal of Manufacturing Science and Engineering* 133:064501–64504.
[165] Magee CL (1966) *Transformation Kinetics, Microplasticity and Aging of Martensite in Fe–31Ni*, (PhD thesis) Carnegie Mellon University, Pittsburgh, USA.
[166] Makinde A, Thibodeau L, Neale KW (1992) Development of an Apparatus for Biaxial Testing for Cruciform Specimens. *Experimental Mechanics* 32:138–144.
[167] Marciniak Z (1961) Influence of the Sign Change of the Load on the Strain Hardening Curve of a Copper Test Subject to Torsion. *Archiwum Mechaniki Stosowanj* 13:743–751.
[168] Marciniak Z, Kuczinski K (1967) Limit Strains in the Processes of Stretch-Forming Sheet Metal. *International Journal of Mechanical Science* 9:609–620.
[169] Marciniak Z, Kuczynski K, Pokota T (1973) Influence of the Plastic Properties of a Material on the Forming Limit Diagram for Sheet Metal in Tension. *International Journal of Mechanical Science* 15:789–805.
[170] Marin J, Hu LW, Hamburg JF (1953) Plastic Stress–Strain Relations of Alcoa 14S-T6 for Variable Biaxial Stress Ratios. *ASM Transactions* 45:686–709.
[171] McClintock FA (1971) Plasticity Aspects of Fracture. Leibowitz H, (Ed.) *Fracture*, vol. 3. Academic Press, USA.
[172] McDowell DL (1985) A Two Surface Model for Transient Non-Proportional Cyclic Plasticity: Part 1. Development of Appropriate Equations. *ASME Journal of Applied Mechanics* 52:298.
[173] Mediavilla J, Peerlings RHJ, Geers MGD (2006) A Nonlocal Triaxiality-Dependent Ductile Damage Model for Finite Strain Plasticity. *Computer Methods in Applied Mechanics and Engineering* 195:4617–4634.
[174] Menzel A, Steinmann P (2001) A Theoretical and Computational Framework for Anisotropic Continuum Damage Mechanics at Large Strains. *International Journal of Solids and Structures* 38:9505–9523.
[175] Merklein M, Biasutti M (2011) Forward and Reverse Simple Shear Test Experiments for Material Modelling in Forming Simulations. *Steel Research International* 702–707.
[176] Merklein M, Biasutti M (2013) Development of a Biaxial Tensile Machine for Characterization of Sheet Metals. *Journal of Materials Processing Technology* 213:939–946.
[177] Merklein M, Hußnätter W, Geiger M (2008) Characterization of Yielding Behavior of Sheet Metal Under Biaxial Stress Condition at Elevated Temperatures. *CIRP Annals – Manufacturing Technology* 57(1):269–274.
[178] Merklein M, Kuppert A (2009) A Method for the Layer Compression Test Considering the Anisotropic Material Behaviour. *International Journal of Material Forming* 12:483–486.
[179] Merklein M, Kuppert A, Geiger M (2010) Time Dependent Determination of Forming Limit Diagrams. *CIRP Annals – Manufacturing Technology* 59(1):295–298.
[180] Merklein M, Lechler J (2006) Investigation of the Thermo-Mechanical Properties of Hot Stamping Steels. *Journal of Materials Processing Technology* 177:452–455.
[181] Merklein M, Lechler J, Geiger M (2006) Characterisation of the Flow Properties of the Quenchenable Ultra High Strength Steel 22MnB5. *CIRP Annals – Manufacturing Technology* 55(1):229–236.
[182] Merklein M, Lechler J, Godel V, Bruschi S, Ghiotti A, Turetta A (2007) Mechanical Properties and Plastic Anisotropy of the Quenchable High Strength Steel 22MnB5 at Elevated Temperatures. *Key Engineering Materials* 344:79–86.
[183] Meyer LW, Zillmann B, Halle T, Lampke T (2010) *Experimental Determination and Strain Rate Sensitivity of the Yield Surface on Different Sheet Metals*, Verformungskundliches Kolloquium, Leoben. ISBN/ISSN 978-3-902078-14-8.
[184] Mises R (1913) Mechanics of Solids in Plastic State. *Göttinger Nachrichten Mathematical Physics* 4:582–592. (in German).
[185] Miyauchi K (1984) Stress–Strain Relationship in Simple Shear of In-Plane Deformation for Various Steel Sheets Efficiency in Sheet Metal Forming. *Proc. of IDDRG*, 360–371.
[186] Muscat-Fenech CM, Arndt S, Atkins AG (1996) The Determination of Fracture Forming Limit Diagrams from Fracture Toughness. *Proc. of Sheet Metal Conference I*, 248–260.
[187] Nahshon K, Hutchinson JW (2008) Modification of the Gurson Model to Shear Failure. *European Journal of Mechanics A/Solids* 27:1–17.
[188] Nazzal MA, Khraisheh MK, Darras BM (2004) Finite Element Modelling and Optimization of Superplastic Forming Using Variable Strain Rate Approach. *Journal of Materials Engineering and Performance* 13:691–699.
[189] Needleman A, Tvergaard V (1984) Limits to Formability in Rate-Sensitive Metal Sheets. *Proc of 4th ICM*, 51–65.
[190] Noman M, Clausmeyer T, Barthel C, Svendsen B, Huetink J, van Riel M (2010) Experimental Characterization and Modelling of the Hardening Behaviour of the Steel Sheet LH800. *Materials Science and Engineering A* 527:2515–2526.
[191] Oyane M (1972) Criteria of Ductile Fracture Strain. *Bulletin of JSME* 15:1507–1513.
[192] Pardoen T, Hutchinson JW (2000) An Extended Model for Void Growth and Coalescence. *Journal of the Mechanics and Physics of Solids* 48(12):2467–2512.
[193] Pawelski O (1967) Über das Stauchen von Hohlzylindern und seine Eignung zur Bestimmung der Formänderungsfestigkeit dünner Bleche. *Archiv für Eisenhüttenwensen* 38:437–442.
[194] Pellegrini D, Ghiotti A, Bruschi S (2011) Effect of Warm Forming Conditions on AZ31B Flow Behaviour and Microstructural Characteristics. *International Journal of Material Forming* 4:155–161.
[195] Prager W (1956) A New Method of Analysing Stresses and Strains in Work-Hardening Plastic Solids. *ASME Journal of Applied Mechanics* 23:493–496.
[196] Rabotnov YN (1963) *On the Equation of State for Creep. Progress in Applied Mechanics – The Prager Anniversary*, The Macmillan Company, New York, NY307–315.
[197] Ramazani A, Abbasi M, Prahl U, Bleck W (2012) Failure Analysis of DP600 Steel Dduring the Cross-Die Test. *Computational Materials Science* 64:101–105.
[198] Ramezani M, Mohd Ripin Z (2010) Combined Experimental and Numerical Analysis of Bulge Test at High Strain Rates Using Split Hopkinson Pressure Bar Apparatus. *Journal of Materials Processing Technology* 210:1061–1069.

[199] Rauch EF (1992) The Flow Law of Mild Steel Under Monotonic or Complex Strain Path. *Solid State Phenomena* 23(24):317–334.

[200] Rauch EF (1998) Plastic Anisotropy of Sheet Metals Determined by Simple Shear Tests. *Materials Science and Engineering A* 241:179–183.

[201] Reisner G, Werner EA, Fischer FD (1998) Micromechanical Modelling of Martensitic Transformation in Random Microstructures. *International Journal of Solids and Structures* 35(17):2457–2473.

[202] Rice JR, Tracey DM (1969) On the Ductile Enlargement of Voids in Triaxial Stress Fields. *Journal of Mechanics and Physics of Solids* 17:201–217.

[203] Rousselier G (1987) Ductile Fracture Models and Their Potential in Local Approach of Fracture. *Nuclear Engineering and Design* 105:97–111.

[204] Rousselier G, Barlat F, Yoon JW (2009) A Novel Approach for Anisotropic Hardening Modelling. Part I: Theory and its Application to Finite Element Analysis of Deep Drawing. *International Journal of Plasticity* 25:2383–2409.

[205] Sato K, Yoshida T, Ando T, Shikida M, Kuwabata T (1998) Tensile Testing of Silicon Film Having Different Crystallographic Orientations Carried out on a Silicon Chip. *Sensors and Actuators A: Physical* 70(1–2):148–152.

[206] Silva MB, Nielsen PS, Bay N, Martins PAF (2011) Failure Mechanisms in Single-Point Incremental Forming of Metals. *International Journal of Advanced Manufacturing Technology* 56:893–903.

[207] Simons G, Weippert C, Dual J, Villain J (2006) Size Effects in Tensile Testing of Thin Cold Rolled and Annealed Cu Foils. *Materials Science and Engineering A* 416(1–2):290–299.

[208] Sokolowski T, Gerke K, Ahmetoglu M, Altan T (2000) Evaluation of Tube Formability and Material Characteristics: Hydraulic Bulge Testing of Tubes. *Journal of Materials Processing Technology* 98:34–40.

[209] Soyarslan C, Malekipour Gharbi M, Tekkaya AE (2012) A Combined Experimental Numerical Investigation of Ductile Fracture in Bending of a Class of a Ferritic-Martensitic Steel. *International Journal of Solids and Structures* 49:1608–1626.

[210] Storen S, Rice JR (1975) Localized Necking in Thin Sheets. *Journal of the Mechanics and Physics of Solids* 23:421–441.

[211] Stoughton TB (2000) A General Forming Limit Criterion for Sheet Metal Forming. *International Journal of Mechanical Sciences* 42:1–27.

[212] Swift HW (1952) Plastic Instability Under Plane Stress. *Journal of the Mechanics and Physics of Solids* 1:1–18.

[213] Taebi F, Demir OK, Stiemer M, Psyk V, Kwiatkwoski L, Brosius A, Blum H, Tekkaya AE (2012) Dynamic Forming Limits and Numerical Optimization of Combined Quasi-Static and Impulse Metal Forming. *Computational Materials Science* 54:293–302.

[214] Taleb L, Cavallo N, Waeckel F (2001) Experimental Analysis of Transformation Plasticity. *International Journal of Plasticity* 17(1):1–20.

[215] Taleb L, Petit S (2006) New Investigation on Transformation Induced Plasticity and its Interaction with Classical Plasticity. *International Journal of Plasticity* 22:110–130.

[216] Tasan CC, Hoefnagels JPM, Dekkers ECA, Geers MGD (2012) Multi-Axial Deformation Setup for Microscopic Testing of Sheet Metal to Fracture. *Experimental Mechanics* 52:669–678.

[217] Tasan CC, Hoefnagels JPM, Quaak G, Geers MGD (2008) In-Plane Biaxial Loading of Sheet Metal until Fracture. in Proulx T, (Ed.) *Proceedings of the 11th International Congress and Exhibition on Experimental and Applied Mechanics*, 1729–1736.

[218] Taylor B (2006) Formability Testing of Sheet Metals. *ASM Handbook Volume 14B Metalworking: Sheet Forming (ASM International)*, 673–696.

[219] Teodosiu C, Hu Z (1995) Evolution of the Intergranular Microstructure at Moderate and Large Strains: Modelling and Computational Significance. *Proc. of Numiform*, 173–182.

[220] Tekkaya A, Pöhlandt K, Dannenmann E (1982) a. Methoden zur Bestimmung derFließkurven von Blechwerkstoffen. – Ein Überblick, Teil I. *Blech Rohre Profile* 29(9):354–359.

[221] Tekkaya AE, Pöhlandt K, Lange K (1982) Determining Stress–Strain Curves of Sheet Metal in the Plane Torsion Test. *CIRP Annals – Manufacturing Technology* 40(1):171–174.

[222] Thuramalla N, Khraisheh M (2004) Multiscale-Based Optmization of Superplastic Forming. *Transactions of NAMRI/SME* 32:637–643.

[223] Tomita Y, Iwamoto T (2001) Computational Prediction of Deformation Behavior of TRIP Steels Under Cyclic Loading. *International Journal of Mechanical Sciences* 43(9):2017–2034.

[224] Toros S, Ozturk F, Kacar I (2008) Review of Warm Forming of Aluminium–Magnesium Alloys. *Journal of Materials Processing Technology* 207:1–12.

[225] Tresca H (1864) On the Yield of Solids at High Pressures. *Comptes Rendus Academie des Sciences* 59:754. (in French).

[226] Turetta A, Bruschi S, Ghiotti A (2006) Investigation of 22MnB5 Formability in Hot Stamping Operations. *Journal of Materials Processing Technology* 177:396–400.

[227] Tvergaard V (1982) On Localization in Ductile Materials Containing Spherical Voids. *International Journal of Fracture* 18:237–252.

[228] Tvergaard V, Needleman A (1984) Analysis of Cup–Cone Fracture in a Round Tensile Bar. *Acta Materialia* 32:157–169.

[229] Uthaisangsuk V, Prahl U, Bleck W (2011) Modelling of Damage and Failure in Multiphase High Strength DP and TRIP Steels. *Engineering Fracture Mechanics* 78:469–486.

[230] Vacher P, Haddad A, Arrieux R (1999) Determination of the Forming Limit Diagrams Using Image Analysis by the Correlation Method. *CIRP Annals – Manufacturing Technology* 48(1):227–230.

[231] Vegter H, Drent P, Huetink J (1995) A Planar Isotropic Yield Criterion Based on Material Testing at Multi-Axial Stress States. in Shen S-FDawson PR, (Eds.) *Simulation of Materials Processing: Theory, Methods and Applications*, Rotterdam, Balkema.

[232] Vegter H, van den Boogaard AH (2006) A Plane Stress Yield Function for Anisotropic Sheet Material by Interpolation of Biaxial Stress States. *International Journal of Plasticity* 22:557–580.

[233] Verleysen P, Peirs J, Van Slycken J, Faes K, Duchene L (2011) Effect of Strain Rate on the Forming Behaviour of Sheet Metals. *Journal of Materials Processing Technology* 211:1457–1464.

[234] Voce E (1955) A Practical Strain Hardening Function. *Metallurgia* 51(307):219–226.

[235] Volk W, Hoffmann H, Suh J, Kim J (2012) Failure Prediction for Non Linear Strain Paths in Sheet Metal Forming. *CIRP Annals – Manufacturing Technology* 61(1):259–262.

[236] Voyiadjis GZ, Abu Al-Rub RK, Palazotto AN (2004) Thermodynamic Formulations for Non-Local Coupling of Viscoplasticity and Anisotropic Viscodamage for Dynamic Localization Problems Using Gradient Theory. *International Journal of Plasticity* 20:981–1038.

[237] Wagoner RH, Wang W, Sriram S (1994) Development of OSU Formability Test and OSU Friction Test. *Journal of Materials Processing Technology* 45(1–4):13–18.

[238] Woodthrope J, Pearce R (1970) The Anomalous Behaviour of Aluminium Sheet Under Balanced Biaxial Tension. *International Journal of Mechanical Sciences* 12:341–347.

[239] *Cruciform Multiaxial Mechanical Testing – Center for Automotive Lightweighting*, (2013), The National Institute of Standards and Technology. www.nist.gov/lighweighting/cruciform-multiaxial-testing.cfm.

[240] Xiao Y, Chen J, Cao J (2012) A Generalized Thermodynamic Approach for Modelling Nonlinear Hardening Behaviours. *International Journal of Plasticity* 38:102–122.

[241] Yamamoto H (1978) Conditions for Shear Localization in the Ductile Fracture of Void-Containing Materials. *International Journal of Fracture* 14:347.

[242] Yin Q, Brosius A, Tekkaya AE (2011) Modified Plane Torsion Tests for Sheet Metal Characterization. *Steel Research International Special Issue ICTP 2011*, Aachen, 696–701.

[243] Yin Q, Soyarslan C, Güner A, Brosius A, Tekkaya AE (2012) A Cyclic Twin Bridge Shear Test for the Identification of Kinematic Hardening Parameters. *International Journal of Mechanical Sciences* 59:31–43.

[244] Yoshida K, Kuwabara T, Kuroda M (2007) Path-Dependence of the Forming Limit Stresses in a Sheet Metal. *International Journal of Plasticity* 23:361–384.

[245] Yoshida K, Kuwabara T, Narihara K, Takahashi S (2005) Experimental Verification of the Path-Dependence of Forming Limit Stresses. *International Journal of Forming Processes* 8:283–298.

[246] Yoshida F, Uemori T (2002) A Model of Large-Strain Cycle Plasticity Describing the Bauschinger Effect and Work Hardening Stagnation. *International Journal of Plasticity* 18:661.

[247] Yoshida F, Uemori T, Fujiwara K (2002) Elastic-Plastic Behaviour of Steel Sheets Under In-plane Cyclic Tension-Compression at Large Strain. *International Journal of Plasticity* 18:633–659.

[248] Yoshida F, Urabe M, Toporov VV (1998) Identification of Material Parameters in Constitutive Model for Sheet Metals from Cyclic Bending Tests. *International Journal of Mechanical Science* 40(2–3):237–249.

[249] Zhao KM, Lee JK (2002) Finite Element Analysis of the Three Point Bending of Sheet Metals. *Journal of Materials Processing Technology* 122:6–11.

[250] Zhao LR, Sowerby R, Sklad MP (1996) A Theoretical and Experimental Investigation of Limit Strains in Sheet Metal Forming. *International Journal of Mechanical Sciences* 38:1307–1317.

[251] Ziegler H (1959) A Modification of Prager's Hardening Rule. *Quarterly of Applied Mathematics* 17:55–65.